Received: 1 May 2018 | Revised: 13 July 2018 | Accepted: 2 August 2018

DOI: 10.1002/hbm.24353

WILEY

RESEARCH ARTICLE

Amygdala subnuclei and healthy cognitive aging

Arash Aghamohammadi-Sereshki[1] | Stanislau Hrybouski[1] | Scott Travis[1] | Yushan Huang[2] | Fraser Olsen[2] | Rawle Carter[2] | Richard Camicioli[1,3] | Nikolai V. Malykhin[1,2]

[1]Neuroscience and Mental Health Institute, University of Alberta, Edmonton, Alberta, Canada

[2]Department of Biomedical Engineering, University of Alberta, Edmonton, Alberta, Canada

[3]Division of Neurology, University of Alberta, Edmonton, Alberta, Canada

Correspondence
Nikolai V. Malykhin, Department of Biomedical Engineering, University of Alberta, Edmonton, AB T6G 2V2, Canada.
Email: nikolai@ualberta.ca

Funding information
Canadian Institutes of Health Research (CIHR), Grant/Award Number: MOP115011

Amygdala is a group of nuclei involved in the neural circuits of fear, reward learning, and stress. The main goal of this magnetic resonance imaging (MRI) study was to investigate the relationship between age and the amygdala subnuclei volumes in a large cohort of healthy individuals. Our second goal was to determine effects of the apolipoprotein E (APOE) and brain-derived neurotrophic factor (BDNF) polymorphisms on the amygdala structure. One hundred and twenty-six healthy participants (18–85 years old) were recruited for this study. MRI datasets were acquired on a 4.7 T system. Amygdala was manually segmented into five major subdivisions (lateral, basal, accessory basal nuclei, and cortical, and centromedial groups). The BDNF (methionine and homozygous valine) and APOE genotypes (ε2, homozygous ε3, and ε4) were obtained using single nucleotide polymorphisms. We found significant nonlinear negative associations between age and the total amygdala and its lateral, basal, and accessory basal nuclei volumes, while the cortical amygdala showed a trend. These age-related associations were found only in males but not in females. Centromedial amygdala did not show any relationship with age. We did not observe any statistically significant effects of APOE and BDNF polymorphisms on the amygdala subnuclei volumes. In contrast to APOE ε2 allele carriers, both older APOE ε4 and ε3 allele carriers had smaller lateral, basal, accessory basal nuclei volumes compared to their younger counterparts. This study indicates that amygdala subnuclei might be nonuniformly affected by aging and that age-related association might be gender specific.

KEYWORDS

aging, amygdala subnuclei, apolipoprotein E (APOE), brain-derived neurotrophic factor (BDNF), magnetic resonance imaging

1 | INTRODUCTION

The amygdala (AG), a medial temporal lobe brain structure consisting of at least 13 subnuclei (Freese & Amaral, 2009; Sah, Faber, Lopez De Armentia, & Power, 2003; Yilmazer-Hanke, 2012), has been considered as a heterogenous structure due to its various cytoarchitectonic and functional features as well as its diverse developmental origin (Freese & Amaral, 2009; LeDoux, 2007; Sah et al., 2003; Yilmazer-Hanke, 2012). The AG is involved in emotional, social, (Adolphs, 2009), and goal-directed (Hampton, Adolphs, Tyszka, & O'Doherty, 2007) behaviors, as well as motivation, explicit memory (LeDoux, 2007), attention, and perception (Vuilleumier, 2009).

Postmortem studies revealed that pathological age-related changes such as the formation of neurofibrillary tangles and neuritic plaques were present in the AG, as well as in the hippocampus and entorhinal cortex (Wright, 2009). However, age-related changes in the AG have been less studied compared to the hippocampus and entorhinal cortex (Allen, Bruss, Brown, & Damasio, 2005; Fjell & Walhovd, 2010). Previous magnetic resonance imaging (MRI) studies of healthy aging reported modest age-related AG atrophy (Brierley, Shaw, & David, 2002; Fjell & Walhovd, 2010; Mather, 2016; Raz & Rodrigue, 2006; Wright, 2009). Furthermore, several studies demonstrated that deleterious effects of aging on the AG volume might not be only cumulative, but also progressive, and become evident after the age of 60 (Grieve, Korgaonkar, Clark, & Williams, 2011; Mu, Xie, Wen, Weng, & Shuyun, 1999), suggesting a nonlinear association between the AG volume and age. However, the underlying neuroanatomical sources of this age-related atrophy are not clear (Wright,

2009), as most of the previous MRI studies measured the AG as a single structure (Bonilha, Kobayashi, Cendes, & Min Li, 2004; Malykhin, Bouchard, Camicioli, & Coupland, 2008; Matsuoka et al., 2003; Pruessner, Collins, Pruessner, & Evans, 2001; Sublette et al., 2008). Recent technological advances in MRI, due to improvements in spatial resolution and tissue contrast (Duyn, 2012), made it possible to delineate the AG subnuclei *in vivo* (Aghamohammadi-Sereshki, Huang, Olsen, & Malykhin, 2018; Entis, Doerga, Barrett, & Dickerson, 2012; Saygin et al., 2017; Tyszka & Pauli, 2016). Despite the fact that specific functions of the human AG subnuclei have not yet been identified (LeDoux & Schiller, 2009), differences in sensory input/output between the AG subnuclei may underlie their functional role (Freese & Amaral, 2009; LeDoux, 2007; Yilmazer-Hanke, 2012). Moreover, sexual hormone markers showed a wide distribution in most of the AG subnuclei in both human and nonhuman primates (Blurton-Jones, Roberts, & Tuszynski, 1999; Österlund, Gustafsson, Keller, & Hurd, 2000a; 2000b; Roselli, Klosterman, & Resko, 2001), suggesting possibility of sex-related differences in the effects of aging on the AG and its subnuclei. However, most of previous age-related studies of the AG did not investigate sexual dimorphism (Heckers, Heinsen, Heinsen, & Beckmann, 1990; Laakso et al., 1995; Malykhin et al., 2008; Mu et al., 1999) or were limited by small sample sizes or narrow age range to find such an effect (Pruessner et al., 2001; Sublette et al., 2008).

Multiple factors, often called modifiers, including genetic, cardiovascular, lifestyle, physical, and cognitive activities can contribute to the interindividual variability observed in studies of healthy brain aging (Fjell & Walhovd, 2010; Raz, Ghisletta, Rodrigue, Kennedy, & Lindenberger, 2010; Raz & Rodrigue, 2006). Therefore, a better understanding of these modifiers and their effects on the human brain is critical (Fjell & Walhovd, 2010; Raz & Rodrigue, 2006). AG is one of the brain structures affected in Alzheimer's and Parkinson's diseases, the two most common neurodegenerative diseases (Braak et al., 1994; Casey, 2013; Harding, Stimson, Henderson, & Halliday, 2002; Krasuski et al., 1998; Scott, DeKosky, Sparks, Knox, & Scheff, 1992). Moreover, the apolipoprotein E (APOE) and brain-derived neurotrophic factor (BDNF) are the two most common genetic polymorphisms that have been investigated in a number of neuroimaging studies due to their associations with Alzheimer's disease, neuronal repair, protection and proliferation, and synaptic growth and memory function (Deary, Wright, Harris, Whalley, & Starr, 2004; Petrella, Mattay, & Doraiswamy, 2008). A better understanding of APOE and BDNF-related effects on healthy aging of the AG might help us to understand protective and/or susceptible factors and mechanisms involved in neurodegenerative diseases.

APOE polymorphism has three known allelic variants ($\varepsilon 2$, $\varepsilon 3$, and $\varepsilon 4$) (Petrella et al., 2008). Previous PET studies reported lower rates of glucose metabolism in posterior cingulate, parietal, temporal, and prefrontal cortex either in the late-middle-aged $\varepsilon 4$ carriers (Reiman et al., 1996) or in relatively young adult $\varepsilon 4$ carriers (Reiman et al., 2004). Moreover, volumetric MRI studies found $\varepsilon 4$-related volumetric atrophy in the AG in Alzheimer's disease (Basso et al., 2006; Hashimoto et al., 2001) and in nondemented older adults (Honea, Vidoni, Harsha, & Burns, 2009).

The role of BDNF in healthy brain aging has also been a subject of many studies (Petrella et al., 2008). A common BDNF polymorphism is an amino-acid substitution of valine (Val) to methionine (Met) at amino-acid residue 66 (Val66Met). The BDNF is expressed throughout the brain and abundantly in the hippocampus and the prefrontal cortex (Petrella et al., 2008). Consequently, most of the previous MRI studies of the BDNF polymorphism focused on those two structures. However, the number of studies investigating the effects of APOE and BDNF polymorphisms on the AG in healthy subjects is very limited (den Heijer et al., 2002; Hibar et al., 2015; Soldan et al., 2015; Sublette et al., 2008) and their effects on the AG subnuclei have not been studied so far.

Therefore, the primary goal of this study was to investigate the nature of the AG subnuclei associations with age in a large sample of healthy individuals across the entire adult lifespan using recently developed ultra-high-resolution MRI volumetric method (Aghamohammadi-Sereshki et al., 2018). Our second goal was to determine effects of APOE and BDNF polymorphisms on the AG and its subnuclei volumes.

2 | MATERIALS AND METHODS

2.1 | Participants

Originally, 140 individuals (62 men and 78 women) were recruited through online, poster, and local advertisements. However, 14 participants were later excluded from the initial sample because of contraindications to the 4.7 T scan or because of difficulty in remaining still during the scanning procedure. Therefore, the final sample consisted of 126 healthy volunteers (58 males and 68 females), between 18 and 85 years of age (mean: 47.6, *SD*: 18.9). Of those, 96 participants were Caucasian (76.2%), 23 Asian (18.2%), and 7 Latin American (5.6%).

An initial phone interview was conducted to screen candidates for existing neuropsychiatric disorders and MRI contraindications. Participants were excluded if they or their first-degree relatives had any history of psychiatric disorders, as assessed by the Anxiety Disorders Interview Schedule—IV (Brown, Di Nardo, Lehman, & Campbell, 2001). The exclusion criteria were active and inactive medical conditions that may interfere with normal cognitive function (cerebrovascular pathology, tumors or congenital malformations of the nervous system, diabetes, multiple sclerosis, neurodegenerative diseases, epilepsy, dementia, and stroke), and use of psychotropics medications and nonprescribed substances that could affect brain function. Most of the individuals were right handed (R: 114; L: 12). Handedness was assessed using a 20-item Edinburgh Handedness Inventory and individuals with laterality quotient ≥+80 were determined as right handed (Oldfield, 1971).

A face-to-face interview was conducted to verify that our older volunteers retained healthy cognitive function. Older subjects (>50 years of age) with mild cognitive impairment and dementia were excluded from the study. For exclusion, dementia was defined according to the DSM-IV criteria. Mild cognitive impairment was defined based on presence of cognitive complaints (documented on the AD-8, Galvin, Roe, Coats, & Morris, 2007) with documented impairment on

the Montreal Cognitive Assessment Test (MOCA) (all included subjects had MOCA score ≥ 26) (Nasreddine et al., 2005). Furthermore, older participants (>50 years of age) were assessed for vascular dementia with the Hachinski Ischemic Scale (HIS) (Hachinski et al., 1975). A score above 7 out of 18 has 89% sensitivity (Moroney et al., 1997). All elderly participants included in this study received a HIS score of 3 or lower.

The Clinical Dementia Rating scale (CDR) was used as an assessment of dementia symptom severity (Hughes, Berg, Danziger, Coben, & Martin, 1982), where subjects are assessed for functional performance in six areas: memory, orientation, judgment & problem solving, community affairs, home and hobbies, and personal care. We employed CDR as an additional screening measure for dementia in older participants. A composite score from 0 to 3 was calculated. All our subjects met the cutoff score of <0.5 for total CDR score. To screen older participants for depression, the Geriatric Depression Scale (GDS) was used (Yesavage et al., 1982). Designed to rate depression in the elderly, a score of >5 is suggestive of depression and a score >10 is indicative of depression. Our subjects met the cutoff score of 4 and below.

Written, informed consent was obtained from each participant. The study was approved by the University of Alberta Health Research Ethics Board.

2.2 | MRI acquisition and data analysis

Imaging was performed on a 4.7 T Varian Inova MRI system at the Peter Allen MR Research Centre (University of Alberta, Edmonton, AB). A T_2-weighted fast spin echo (FSE) sequence [TE: 39 ms; TR: 11,000 ms; bandwidth: 34.97 kHz; echo spacing: 19.5 ms; echo train length: 4; FOV: 20 × 20 cm; native resolution: 0.52 × 0.68 × 1.0 mm^3] was utilized with contiguous 1-mm-thick slices and a 90° excitation followed by a 160° and three 140° refocusing pulses. In total, 90 slices were attained perpendicular to the anterior–posterior commissure (AC–PC) line in a total acquisition time of 13.5 min. All high-resolution FSE images were reconstructed and inspected for motion artifacts while the subject was in the scanner, allowing a second or a third FSE dataset to be collected if required. A whole brain T_1-weighted 3D MPRAGE sequence [TR: 8.5 ms; TE: 4.5 ms; inversion time: 300 ms; flip angle: 10°; bandwidth: 80 kHz; FOV: 256 × 200 × 180 mm^3; voxel size: 1 × 1 × 1 mm^3] was acquired for intracranial volume (ICV) estimation. FSE images were interpolated in-plane by a factor of 2 to yield a final resolution of 0.26 × 0.34 × 1.0 mm^3 and voxel volume of 0.09 μL. DISPLAY (Montreal Neurological Institute, QC, Canada) software was used to trace the ICV, and all AG ROIs. Three-dimensional models of the AG and its subnuclei were created using ITK-SNAP software (v. 3.6.0; Yushkevich et al., 2006).

Detailed reliable protocols for the manual tracing of the total AG (Malykhin et al., 2007) and AG subnuclei (Aghamohammadi-Sereshki et al., 2018) were previously reported in detail. The AG was manually segmented using geometrical rules that approximately match the location and orientation of the AG subnuclei based on histological references (Brabec et al., 2010; García-Amado & Prensa, 2012; Mai et al., 2008; Schumann & Amaral, 2005). Total AG was manually traced from the most posterior slice continued through slices where both the AG and hippocampal head were present and ended at the level of sulcus closure (Malykhin et al., 2007). Subsequently, only the coronal plane was used to segment the AG into its five major subnuclei groups: the lateral (La) nucleus, the basal (B) nucleus, the accessory basal (AB) nucleus (these three nuclei form the basolateral group [BLA]), the cortical (Co) group, and the centromedial (CeM) group (Figure 1). A single internal landmark line—which was either a horizontal line that connects the most medial border of the AG to the most lateral border of the AG or a diagonal line that connects the most inferomedial border of the AG to the most medio-inferior border of the AG—was used to segment AG into the aforementioned subnuclei groups (Aghamohammadi-Sereshki et al., 2018). Generally, consistent measurements of the AG subnuclei can be obtained by a person experienced in medial temporal lobe anatomy in 2 hr. All measurements were performed by a single rater (A.S.S.) who was blind to all demographic and genotype information. Raw volumetric measurements were adjusted to the ICV by using the following formula: ICV-adjusted volume = [raw ROI volume (mm^3)/ICV of the same individual (cm^3)] × sample average ICV (cm^3) (Malykhin, Huang, Hrybouski, & Olsen, 2017).

Although both total brain volume (TBV) and ICV are frequently used to correct for individual differences in head size (Mankiw et al., 2017; Nordenskjöld et al., 2015; Reardon et al., 2016; Tan, Ma, Vira, Marwha, & Eliot, 2016), we used ICV to normalize the AG volumes because unlike the TBV, ICV does not change with age (Michielse et al., 2010; Raz et al., 2004; Shang, Carlson, & Tang, 2018; Ystad et al., 2009).

The inter-rater reliability was assessed by two raters (A.A.S. and N.V.M.; developers of the AG segmentation protocol), who independently traced the AG and its subnuclei in five subjects (10 amygdalae total). Intra-rater reliability for the total AG and its subnuclei volume measures was assessed by retracing the images from the same five subjects at 1–2 weeks interval by a single rater (A.A.S.) who performed all manual measurements of this study (Table 1). It is important to mention that the MRI scans used to assess the intra/inter-rater reliability were different from the datasets used for training.

2.3 | Genetic analysis

The genotypes for our genes of interest were obtained using single-nucleotide polymorphisms (SNPs) derived from cheek swabs from our participants. Primer3PLUS was used to generate primers using sequence data from dbSNP. Primers were positioned to generate a clean single PCR product with the variant in a position near the center of the read to avoid common technical artifacts that can occur during the sequencing step. All primers were purchased from Integrated DNA Technologies (Coralville, IA). APOE polymorphisms were determined on the basis of two SNPs: rs7412 (C; T), which ancestral nucleotide is C and rs429358 (T; C) which ancestral nucleotide is T. The presence of rs7412-T and rs429358-T indicates an ε2 allele; the presence of rs7412-C and rs429358-T indicates an ε3 allele; and the presence of rs7412-C and rs429358-C indicates an ε4 allele. BDNF polymorphisms were obtained using rs6265(G; A), where the G allele encodes Val and the A allele encodes Met. The BDNF Met zygosity was collapsed into a single group due to few homozygous Met/Met

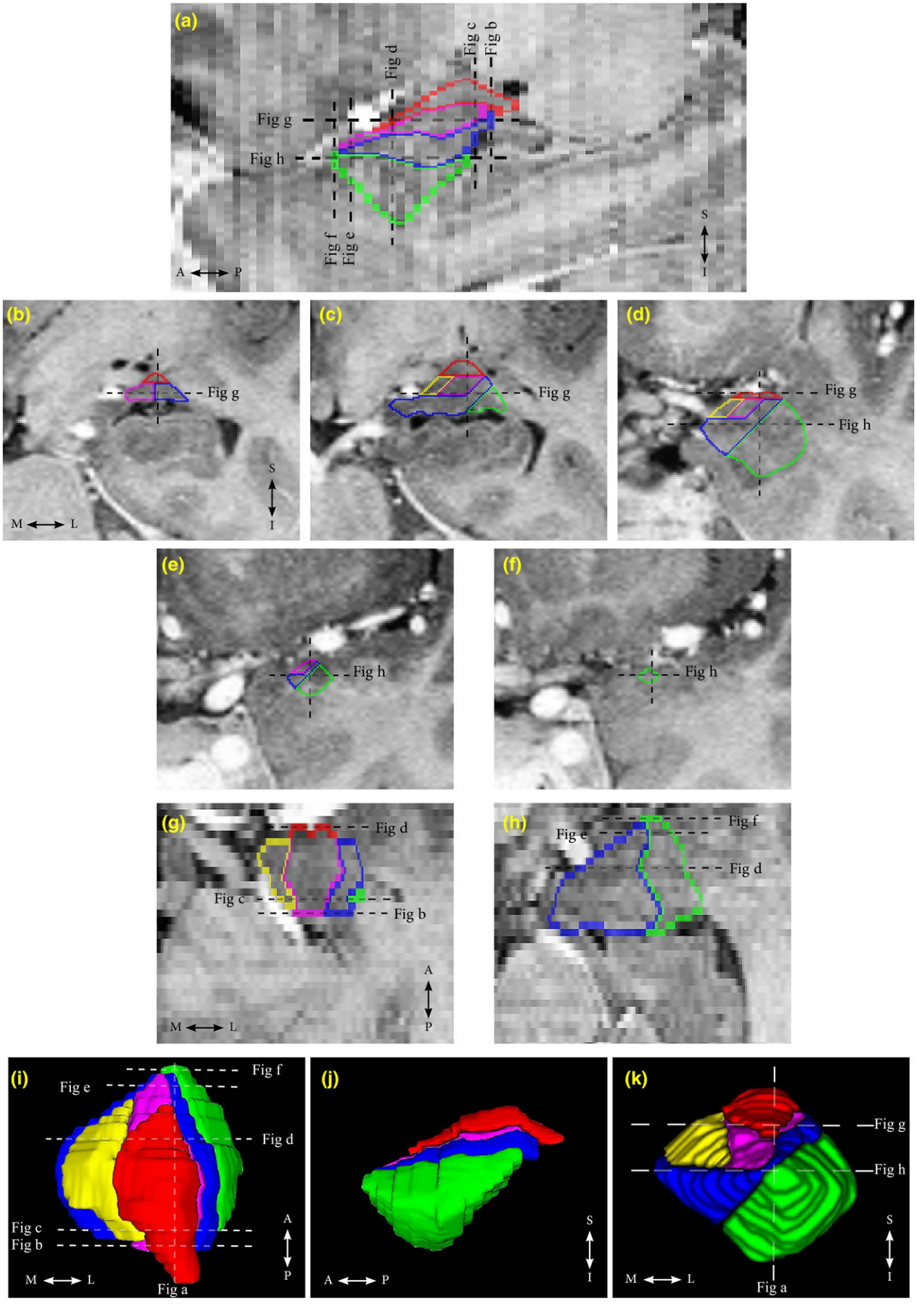
(a)
Fig d
Fig c
Fig b
Fig g
Fig h
Fig f
Fig e
A
P
S
I
(b)
Fig g
S
M
L
I
(c)
Fig g
(d)
Fig g
Fig h
(e)
Fig h
(f)
Fig h
(g)
Fig d
Fig c
Fig b
A
M
L
P
(h)
Fig f
Fig e
Fig d
(i)
Fig f
Fig e
Fig d
Fig c
Fig b
A
M
L
P
Fig a
(j)
S
A
P
I
(k)
Fig g
Fig h
S
M
L
I
Fig a

genotypes (n = 4). For our final analysis, we, therefore, created two groups: Met carriers or "Met/x" (i.e., Met/Val and Met/Met) and homozygous "Val/Val." APOE genotype groups were created according to the presence of either the ε2 or ε4 alleles to test for preservative or deleterious effects. As such, three groups were created for the final analysis: "ε2/x" (ε2 carriers), homozygous "ε3/ε3," and "ε4/x" (ε4 carriers). Participants who possessed both ε2 and ε4 alleles were excluded from the analysis since we observed no statistically significant differences between their inclusion and exclusion, and their frequency was small (n = 3). All genotype frequencies are reported in the results section.

2.4 | Statistics

2.4.1 | Demographic information and descriptive AG volumes analyses

All descriptive and inferential statistics other than regression models for age effects were calculated using IBM SPSS Statistics (Version 24.0 for Windows). Group characteristics such as age, education, and ICV were analyzed by a one-way analysis of variance (ANOVA) and with sex as the independent variable. Moreover, demographic information (sex, age, and education) of BDNF (methionine [met+/+; met +/−] and homozygous valine [+/+] carriers) and APOE (ε2 [ε2/x], homozygous ε3 [ε3/ε3], and ε4 [ε4/x] carriers) polymorphisms were analyzed using a one-way ANOVA. In addition, the chi-squared test was used to evaluate deviation from the Hardy–Weinberg equilibrium. To analyze the effects of genetic polymorphism on the AG volumes, we used a one-way ANOVA with polymorphism as the between-subject factor and the AG ROI volumes as the dependent variables. To avoid independence assumptions inherent to simple Bonferroni-related correction techniques (i.e., absence of any relationship among AG subdivisions' volumes), permutation tests (100,000 shuffles) were used to generate Holm–Bonferroni corrected null distributions when correcting for multiple comparisons [one test for total AG; three tests for CeM, Co, and BLA groups; three tests for subnuclei groups within the BLA group (i.e., La, B, and AB nuclei)].

2.4.2 | Hemispheric effects analysis

A general linear model (GLM) was used to assess the main effect of age and age × sex interaction on asymmetry indices [{[(right volume)/(left volume)} × 100) − 100] as well as the hemispheric effects on the AG ROIs' volumes (within-subjects factor) in males and females (between-subjects factor). As our statistical analyses did not reveal any significant effects of age (all ps > .05) and age × sex interaction (all ps > .14) on AG ROIs' asymmetry indices and significant effect of hemisphere on AG ROIs' volumes (all ps > .29), left and right AG volumetric data were averaged for analyses.

TABLE 1 Reliability results

ICCs and Dice's kappa values				
	ICC		Dice kappa	
	Intrarater	Inter-rater	Intrarater	Inter-rater
La	0.95	0.93	0.86	0.82
B	0.94	0.87	0.81	0.76
AB	0.96	0.95	0.77	0.71
Co	0.97	0.87	0.72	0.72
CeM	0.86	0.85	0.79	0.76
AG	0.93	0.95	0.93	0.91

Note. Abbreviations: AB = accessory basal; AG = amygdala; B = basal; CeM = centromedial; Co = cortical; La = lateral.

2.4.3 | Modeling age relationships for the AG ROIs

Low-order regressions impose severe shape restrictions (e.g., straight line for linear models and a parabola for quadratic models), while higher order functions may lead to overfitting and poor generalizability. Here, we relied on multi-model inference to overcome those limitations. Multi-model inference does not assume that a single model is the "optimal" or "true" fit to the dataset. Instead, each model receives a likelihood estimate and models are subsequently averaged, based on their likelihoods (Burnham & Anderson, 2002; Ziegler et al., 2012). All the ensuing computations were performed using in-house custom-written MATLAB (v. 2016b) programs.

Constructing models that explain the AG ROIs' age relationships

To estimate the relationship between age and the volumetric variations of the total AG and the AG subnuclei in males and females, we first generated a complete set of 16 parameters incorporating age, sex, and age × sex interactions up to polynomial order 5 (1, sex; 2, age; 3, age × sex [male]; 4, age × sex [female]; 5, age^2; 6, age^2 by sex [male]; 7, age^2 by sex [female]; 8, age^3; 9, age^3 × sex [male]; 10, age^3 × sex [female]; 11, age^4; 12, age^4 × sex [male]; 13, age^4 × sex [female]; 14, age^5; 15, age^5 × sex [male]; 16, age^5 × sex [female]). Second, all possible combinations of these parameters were computed to build a complete set of all possible models containing at least one of the aforementioned parameters. Third, models with severe multicollinearity (i.e., containing parameters with variance inflation factor [VIF > 10]) were excluded, as severe multicollinearity can result in complex and unstable regression solutions (Ziegler et al., 2012), and the intercept terms were added to all remaining models. Finally, a single model containing only the intercept term was added to the trimmed model set, to reduce the risk of overfitting in case our data contained no evidence for age- or sex-related effects. The entire model generation produce produced 456 potential polynomial regression models, up to fifth polynomial order, with various combinations of sex, age, and interactions terms (Figure 2).

FIGURE 1 Segmentation of the amygdala (AG) subnuclei on a (a) sagittal, (b–f) coronal, and (g,h) axial views is shown on T_2-weighted FSE images with inverted contrast. Three-dimensional reconstructions of the AG and its subnuclei from a healthy volunteer are shown from (i) the superior, (j) the lateral, and (k) the anterior views. Lateral (La) nucleus is outlined in green, basal (B) nucleus is outlined in dark blue, accessory basal (AB) nucleus is outlined in purple, cortical (Co) group is outlined in yellow, and centromedial (CeM) group is outlined in red. Dashed lines indicate the corresponding slice locations [Color figure can be viewed at wileyonlinelibrary.com]

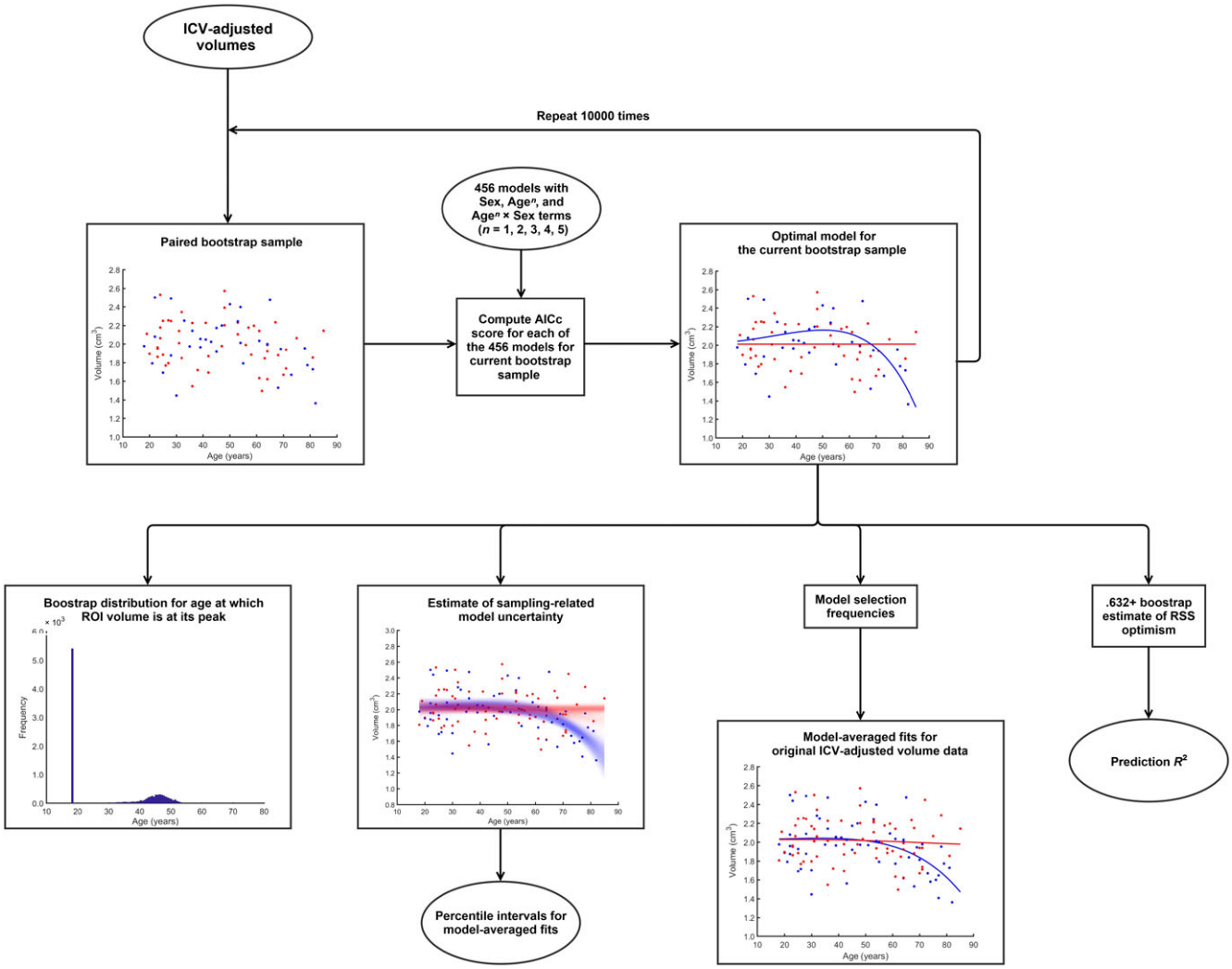

FIGURE 2 Flow chart depicting bootstrap methodology used to model the AG ROIs' relationship to age and their prediction R^2 values [Color figure can be viewed at wileyonlinelibrary.com]

Next, we used nonparametric bootstrap to estimate relative model likelihoods for each of the aforementioned 456 models (Burnham & Anderson, 2002). Model likelihoods were estimated separately for each AG ROI. First, we generated a total of 10,000 paired (i.e., keeping age and volume together) bootstrap samples[1] from the original dataset. For each bootstrap sample, the model with the lowest small-sample Akaike information criterion (AICc) score was selected. As males and females were modeled simultaneously, any sex differences or age × sex interactions were detected automatically by the AICc algorithm. From each bootstrap sample, we built a list of model selection frequencies, which were used as estimates of model likelihood, when computing model-averaged fits for relationships between age and AG ROI volumes in males and in females. Furthermore, as each bootstrap sample generated estimates of AG ROI volumes for the entire age range, we were able to construct 95% percentile intervals around our model-averaged fits. Next, we computed R^2 values for our model-averaged fits, as well as "Prediction R^2" using .632+ bootstrap technique (Efron & Tibshirani, 1997) (Figure 2). These "Prediction R^2" values represent how much of variation in the volumes of the AG ROIs we expect to explain in new data by our model-averaged fits. Traditionally cross-validation techniques have been used for estimating model performance on new data. Although prediction error acquired by *k*-fold cross-validation is fairly accurate, it can be quite variable, requiring repeated random partitioning of the data into different folds, leading to computation constraints for computationally heavy model fitting procedures like ours. The .632+ bootstrap is competitive and can even outperform cross-validation techniques (Efron & Tibshirani, 1997) when estimating out-of-sample residual sum of squares (RSS), but is less computationally demanding than repeated cross-validation.

Finally, age at which AG ROIs' volumes reach maximum volume was estimated for each bootstrap sample. From these, percentile intervals for age at which the AG and the AG subnuclei volumes are at their peak were constructed (Figure 2). The 99% two-tailed thresholds from these percentile intervals were used to partition the data into

[1]*Bootstrapping*: randomly sampling data, with replacement, from the original dataset (i.e., a data point is put back into the original dataset before drawing another data point). Therefore, each data point can be sampled several times or not at all. Each bootstrap sample had the same sample size as the original dataset (see Hesterberg, Moore, Monagham, Clipson, & Epstein, 2009 for further details).

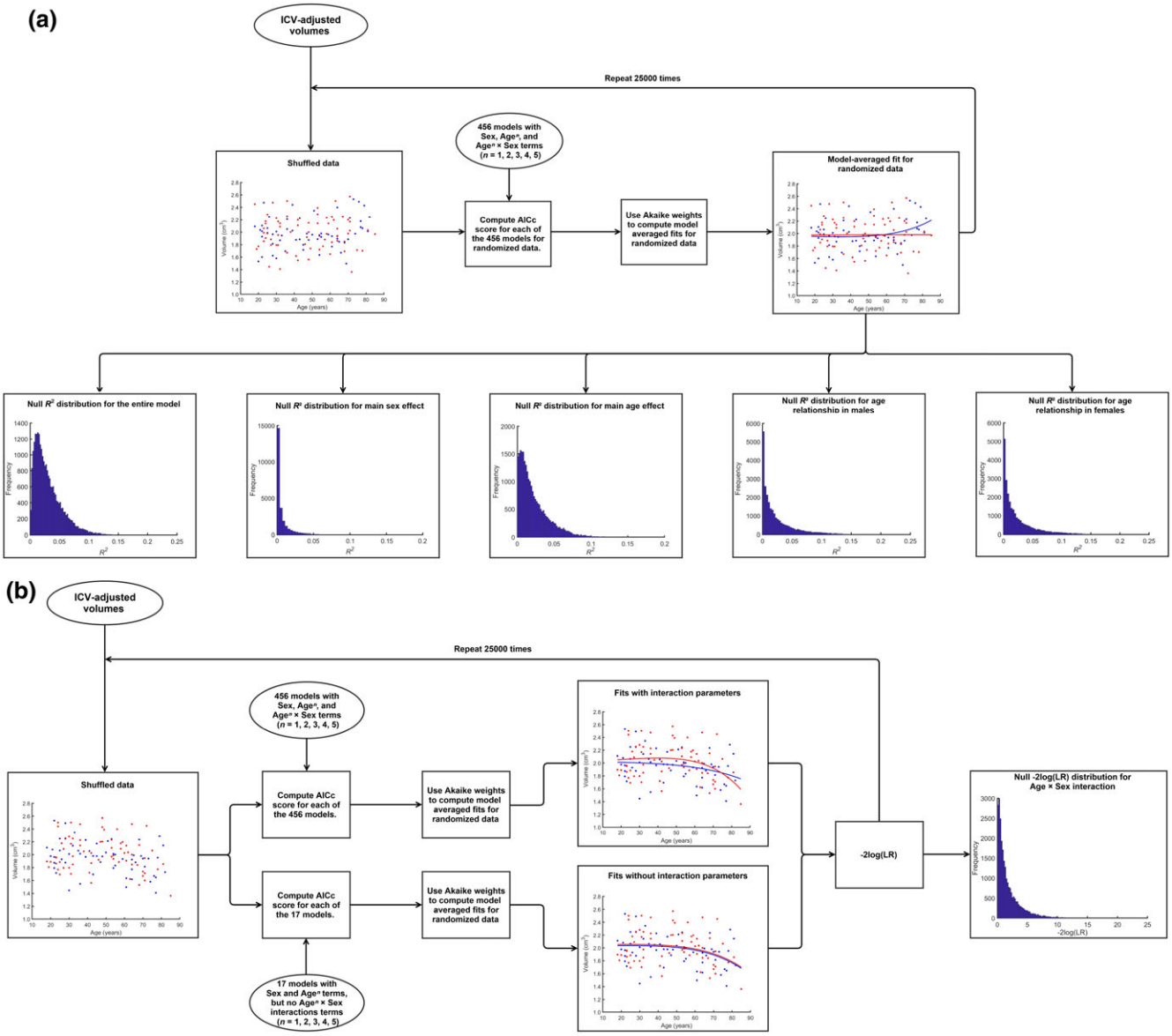

FIGURE 3 Flow chart depicting permutation methodology used to build null distributions to assess the statistical significance of the AG ROIs' (a) overall model significance, age, and sex effects, as well as (b) age by sex interactions. LR: likelihood ratio [Color figure can be viewed at wileyonlinelibrary.com]

two groups: (1) prior to age-related volumetric decline and (2) after the onset of age-related volumetric decline.

Assessing the statistical significance of the AG ROIs' model-averaged regression fits

To evaluate the statistical significance of our model-averaged regression fits, Monte Carlo permutation tests[2] (25,000 simulations) were used to construct "R^2" distributions under the null hypothesis (Figure 3a). It should be noted that due to computational constraints, we were unable to employ resampling techniques to estimate model likelihoods for each of the 25,000 shuffled datasets (it would result in 25,000 × 10,000 × 456 GLM estimations per each AG ROI). Instead, we used a theoretical framework (i.e., Akaike weights), which generally produces similar model likelihoods as bootstrap-based resampling techniques (Burnham & Anderson, 2002). Because the number of effective degrees of freedom is ambiguous when employing model averaging, we used R^2 distributions under the null hypothesis to conduct significance tests. Since the ratio of $R^2/(1 - R^2)$ is proportional to F statistic scores, p values estimated from R^2 distributions under the null hypothesis are mathematically equivalent to p values from F statistic distributions (Moore, McCabe, & Craig, 2009). In total, we simulated five R^2 distributions under the null hypothesis aimed at evaluating the statistical significance of (1) the entire regression model; (2) presence of any relationship between the AG ROI volumes and age, regardless of sex; (3) significance of main sex effects; significance of age relationships in (4) males and (5) females separately (Figure 3a).

[2]*Permutation test*: assessing statistical significance using data randomization. Typically, this involves decoupling of the dependent variable from the independent variable by, for example, randomly assigning data points from the former to the data points of the latter [25,000 shuffles for each ROI in our pipeline]. This generates data samples of any possible association [positive, negative or neutral] between the dependent and independent variables.

TABLE 2 Demographic information

Variable	Male	Female	Total	*F* value	*p* value
Number	58	68	126	–	–
Age in years (mean ± SD)	48.33 ± 19.7	47.13 ± 18.34	47.68 ± 18.91	0.12	.73
Education in years (mean ± SD)	16.26 ± 2.44	15.68 ± 2.44	15.94 ± 2.45	1.78	.18
ICV volume, mean ± SD (cm^3)	1,740.36 ± 136.88	1,520.26 ± 110.75	1,621.57 ± 165.07	99.5	< .0001

Note. Abbreviation: ICV = intracranial volume.

Finally, to assess the statistical significance of age × sex interactions, ROI volume shuffling was restricted to individuals of similar age (age difference < 3 years). Subsequently, AICc model selection with model averaging based on Akaike weights was performed under two sets of criteria: (1) from the entire set of 456 models and (2) from a reduced set of 17 models, containing only main effect terms. For each randomized dataset, the likelihood ratio (LR) for the reduced over full model was computed. These LRs were converted to conventional −2 log(LR) test statistic scores, which, in turn, were used to build the −2 log(LR) distribution under the null hypothesis for age × sex interaction (Figure 3b).

Similar to conventional GLM procedures, we tested for the overall regression significance (i.e., significance of at least one of the following: main age effect, main sex effect, sex-specific age effect) first. These tests revealed the probability that variance explained by age or sex-related effects in the AG ROIs could have arisen due to chance. Next, we tested for significance of age, sex, and interaction effects. Last, we tested whether associations with age were statistically significant in each sex. We applied the Holm–Bonferroni procedure to correct for type I error inflation due to multiple hypothesis testing at the level of regression significance [one test for total AG; three tests for CeM, Co, and BLA groups; three tests subnuclei groups within the BLA group (i.e., La, B, and AB nuclei)]. Similar to factorial designs, no correction for multiple comparisons was used when evaluating the significance of main effects or interactions within each AG ROI. However, a second Holm–Bonferroni correction for multiple comparisons was applied when examining age relationships in each sex separately (two tests for each AG ROI). Finally, we also calculated likelihood ratios (LRs) for model-averaged relative to linear regression fits.

3 | RESULTS

3.1 | Demographics and descriptive statistics

Participants' characteristics for the entire sample is shown in the Table 2. Males had larger ICVs [$F(1, 124) = 99.5$, $p < .0001$] than females while males and females did not differ in age and education (all *p*s > .18) (Table 2). Furthermore, demographic characteristics were not different between carriers of the BDNF genotypes (all *p*s > .23), and between carriers of the APOE genotypes (all *p*s > .08) either in the younger (<55 years old) or in the older (≥55 years old) participants. ICV-adjusted AG and AG subnuclei volumes for the left hemisphere, the right hemisphere, and the average, as well as ICV for the young adults (18–39 years old), the middle age (40–59 years old), and the old adults (≥60 years old) are shown in Table 3.

3.2 | Age and sex effects on the AG ROIs

3.2.1 | Age and sex effects on the total AG

The total AG volume showed a statistically significant relationship to age [$R^2 = .15$, $p < .002$; prediction $R^2 = .06$] (Figure 4), as was the age × sex interaction [$p < .024$]. Consequently, we examined age relationships in males and females separately, which revealed a significant association between the total AG volume and age in males [$R^2 = .25$, $p < .001$; prediction $R^2 = .13$], but not in females [$p > .57$]. However, after controlling for age, males and females had similar ICV-adjusted total AG volume [$p > .60$].

Last, nonlinearity LR for the relationship between total AG volume and age in males was 55.44, indicating that the association between age and total AG volume is likely nonlinear.

3.2.2 | Age and sex effects on the AG subnuclei groups

Next, we investigated how age and sex related to the three major AG subnuclei groups: BLA, Co, and CeM. We found significant association between age and volume of the BLA group [$R^2 = .16$, $p < .001$; prediction $R^2 = .05$], while the Co group showed a trend towards significance for age association [$R^2 = .08$, $p < .092$; prediction $R^2 = 0$]. However, the CeM group did not show any age- or sex-related effects [$p > .48$] (Figure 5). Consequently, the CeM results were not investigated further. Both the BLA and the Co groups showed significant age × sex interaction effects (both *p*s < .050). Analysis of age-related effects in each sex separately revealed that both AG subnuclei groups displayed significant relationships to age in males [BLA: $R^2 = .26$, $p < .001$, prediction $R^2 = .14$; Co: $R^2 = .13$, $p < .021$, prediction $R^2 = .03$], but not in females (both *p*s > .40). No global sex differences, after accounting for age-related effects, were present in any of the AG groups (i.e., BLA, Co, and CeM; all *p*s > 0.50). Nonlinearity LRs for age relationship in males were 35.53 for the BLA group and 10.86 for the Co group.

3.2.3 | Age and sex effects on the BLA AG

Our multi-model regressions between age and BLA nuclei volumes were statistically significant for the La [$R^2 = .12$, $p < .006$; prediction $R^2 = .01$], B [$R^2 = .16$, $p < .002$; prediction $R^2 = .07$], and AB [$R^2 = .12$, $p < .007$; prediction $R^2 = .02$] nuclei (Figure 6). Age × sex interactions were statistically significant for the B and the AB nuclei (both *p*s < .035) and showed a trend toward significance for the La nucleus ($p < .076$). Analyses of age-related effects for each sex separately demonstrated significant associations between age and each of the BLA nuclei in males [La: $R^2 = .22$, $p < .003$, prediction $R^2 = .12$; B: $R^2 = .26$, $p < .001$, prediction $R^2 = .16$; AB: $R^2 = .19$ $p < .003$, prediction $R^2 = .06$,], but not in females (all *p*s > .44). After statistically

TABLE 3 ICV-adjusted AG and its subnuclei volumes (mean ± SD) in young, middle-age, and older adults

AG ROIs (mm^3)		Young adults (18–39 years, *n* = 50)		Middle age (40–59 years, *n* = 35)		Older adults (60–85 years, *n* = 41)	
		Male (*n* = 23)	Female (*n* = 27)	Male (*n* = 15)	Female (*n* = 20)	Male (*n* = 20)	Female (*n* = 21)
La	Left	656.8 ± 100.1	632.0 ± 116.1	669.8 ± 107.4	652.2 ± 91.6	590.8 ± 113.4	639.3 ± 117.8
	Right	641.2 ± 143.6	669.1 ± 138.7	659.6 ± 91.4	650.6 ± 102.4	556.4 ± 141.9	587.9 ± 101.7
	Average	648.9 ± 107.3	650.5 ± 108.7	664.7 ± 82.1	651.4 ± 78.8	573.6 ± 101.3	613.6 ± 92.4
B	Left	622.1 ± 99.4	612.4 ± 104.2	614.0 ± 62.1	641.3 ± 98.1	521.5 ± 89.5	593.6 ± 112.6
	Right	635.4 ± 147.5	630.8 ± 98.7	617.4 ± 85.6	618.1 ± 91.9	512.9 ± 98.5	578.9 ± 86.6
	Average	628.8 ± 113.7	621.6 ± 94.5	615.7 ± 64.9	629.7 ± 83.3	517.2 ± 85.0	586.3 ± 92.6
AB	Left	285.6 ± 44.5	278.8 ± 46.0	285.8 ± 39.6	291.5 ± 43.3	248.8 ± 46.3	269.4 ± 54.1
	Right	280.3 ± 59.2	284.2 ± 40.0	283.3 ± 44.6	282.8 ± 34.2	245.0 ± 53.6	259.5 ± 37.2
	Average	282.9 ± 48.4	281.5 ± 37.6	284.5 ± 38.2	287.1 ± 31.5	246.9 ± 44.4	264.4 ± 38.2
Co	Left	165.7 ± 22.2	163.8 ± 29.6	176.1 ± 39.9	174.6 ± 31.5	153.6 ± 30.6	159.8 ± 30.7
	Right	159.4 ± 33.8	163.3 ± 24.3	159.6 ± 31.8	168.2 ± 23.0	143.3 ± 23.9	153.4 ± 24.7
	Average	162.6 ± 24.7	163.5 ± 21.4	167.8 ± 30.1	171.4 ± 21.6	148.4 ± 22.3	156.6 ± 21.8
CeM	Left	282.0 ± 44.1	292.5 ± 70.4	319.2 ± 90.2	308.9 ± 61.3	291.5 ± 62.3	302.5 ± 67.9
	Right	299.9 ± 66.6	319.2 ± 43.7	303.1 ± 56.8	320.5 ± 56.5	290.9 ± 55.5	301.9 ± 54.3
	Average	291.0 ± 40.3	305.9 ± 47.1	311.1 ± 59.9	314.7 ± 46.6	291.2 ± 40.5	302.2 ± 52.0
Total AG	Left	2,012.2 ± 227.1	1,979.5 ± 253.9	2,065.1 ± 212.6	2,068.6 ± 251.1	1,806.3 ± 268.8	1,964.6 ± 292.2
	Right	2,016.4 ± 376.7	2,066.7 ± 253.8	2,023.5 ± 262.3	2,040.4 ± 242.1	1,748.7 ± 301.0	1,881.8 ± 242.6
	Average	2,014.3 ± 279.8	2,023.1 ± 237.6	2,044.1 ± 219.1	2,054.5 ± 209.1	1,777.5 ± 256.5	1,923.2 ± 242.4
ICV (cm^3)	Average	1,771.9 ± 142.0	1,514.1 ± 126.2	1,752.8 ± 134.6	1,522.2 ± 95.8	1,694.7 ± 126.4	1,526.4 ± 107.5

Note. Abbreviations: AB = accessory basal; AG = amygdala; B = basal; CeM = centromedial; Co = cortical; ICV = intracranial volume; La = lateral; *n* = number of individuals; ROIs = regions of interest.

controlling for age-related effects, ICV-adjusted La, B, and AB nuclei showed no volumetric differences between males and females (all *p*s > .46). Nonlinearity LRs for age relationship in males were 75.85 for the La, 6.94 for the B, and 19.04 for the AB nuclei.

All regression-related results and linear versus nonlinear likelihood ratio estimations are presented in Table 4.

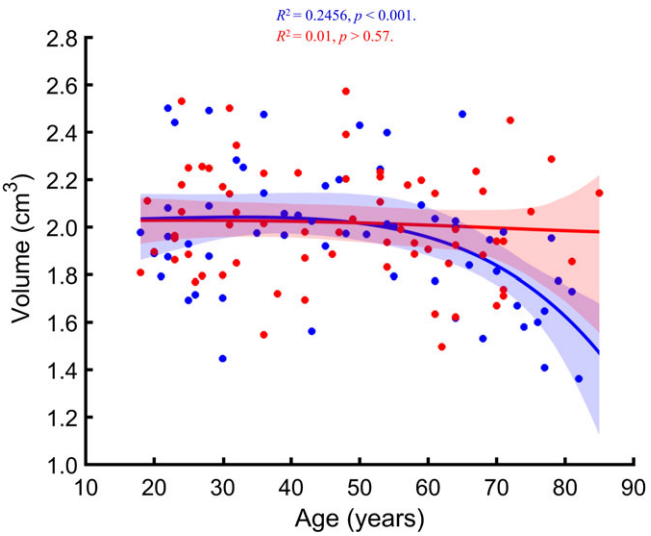

FIGURE 4 Regression plot showing the relationship between age and the ICV-adjusted total AG volume. Model-averaged estimates for men (blue) and women (red) are shown separately. Shaded areas represent the 95% bootstrap percentile confidence interval for each fit [Color figure can be viewed at wileyonlinelibrary.com]

3.3 | Effects of BDNF and APOE genetic polymorphism on the AG

The chi-squared test showed that our sample for both APOE (χ^2 = 5.39, *p* = .37) and BDNF (χ^2 = 0.07, *p* = .97) was in Hardy–Weinberg equilibrium. Also, we observed with a 99% confidence that in all AG subnuclei, which demonstrated significant relationship to age, most of age-related atrophy occurs after the age of 55. Therefore, we divided our sample into two separate groups: (1) prior to age-related volumetric decline (18–54 years) and (2) post-age-related volumetric decline (≥55 years). This categorization allowed us to investigate whether effects of genetic polymorphisms were different in younger or older individuals. The AG ROIs' volumetric analyses did not show any statistically significant differences in any of the AG ROIs' volumes between the carriers of BDNF and between the APOE allelic variants neither in the younger nor in the older groups (all uncorrected *p*s > .08) (Tables 5 and 6). However, volume of the total AG (*p* = .09) in older Met carriers showed a trend towards larger volumes compared to older homozygous Val carriers. Since previous literature indicated that the APOE ε2 allele was associated with positive survival and longevity effects in elderly individuals (Corder et al., 1996; Schächter et al., 1994; Wisdom, Callahan, & Hawkins, 2011), while APOE ε4 allele carriers are more likely to develop the late-onset Alzheimer's disease (Farrer et al., 1997), we also compared AG subnuclei volumes between younger and older carriers of the same allele to determine if age-related volumetric atrophy was present in all APOE allele carriers. Younger and older individuals within each APOE allele did not differ in ICV (all *p*s > .18) or sex (all *p*s > .1). We found that older APOE ε2 allele carriers did not differ in any AG subnuclei volumes from younger counterparts, while both older APOE ε4 allele carriers and

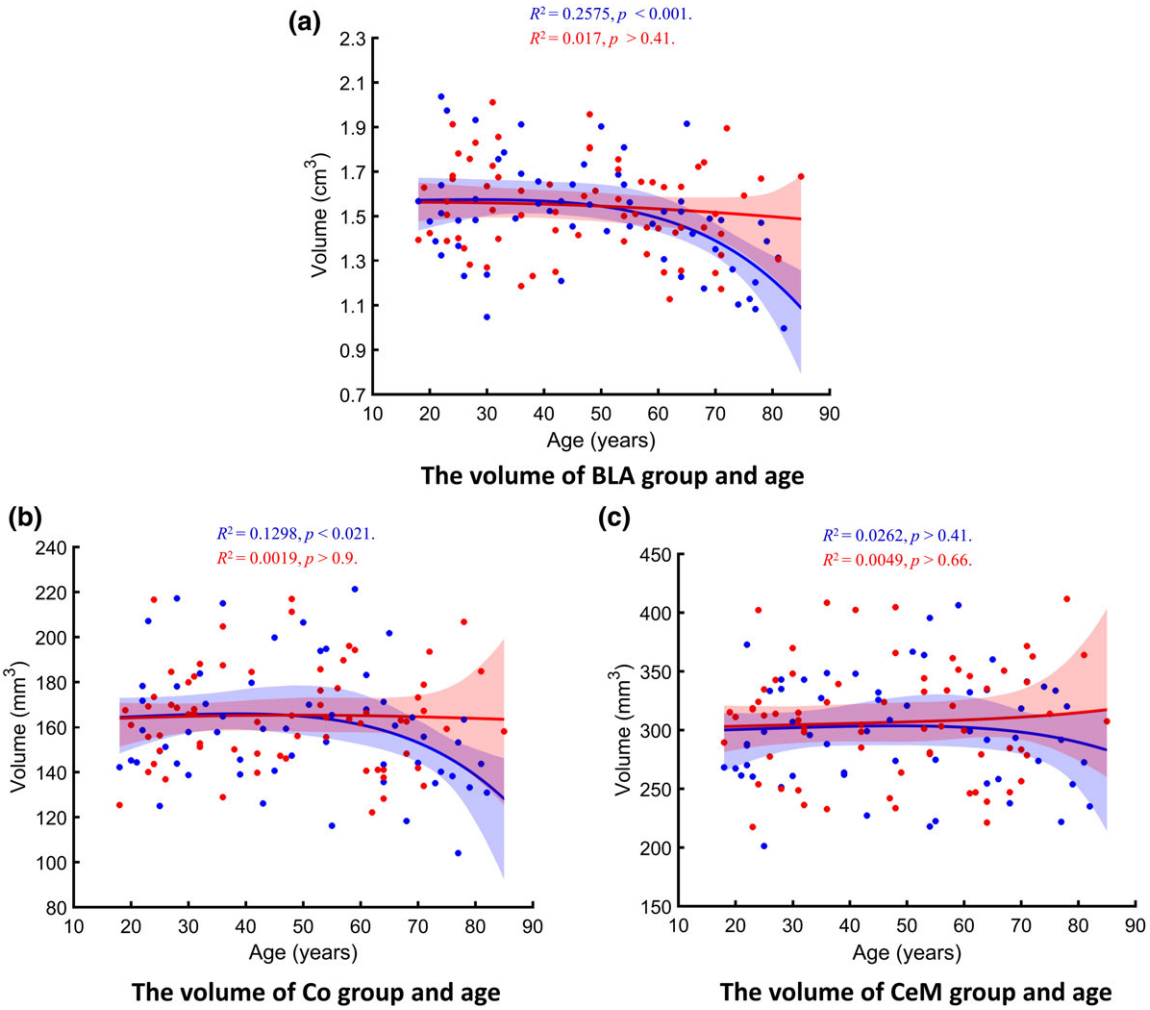

FIGURE 5 Regression plots showing the relationship between age and the ICV-adjusted volumes of the AG subnuclei groups: (a) basolateral (BLA), (b) Co, and (c) CeM subnuclei groups. Model-averaged estimates for men (blue) and women (red) are shown separately. Shaded areas represent the 95% bootstrap percentile confidence interval for each fit. *P* values are corrected for multiple comparisons [Color figure can be viewed at wileyonlinelibrary.com]

older APOE ε3 allele carriers had smaller BLA volumes (with the difference driven by all of its subnuclei; i.e., La, B, AB), which in turn translated to relatively smaller total AG volumes among older APOE ε4 and APOE ε3 allele carriers compared to their younger counterparts. Furthermore, the effect size of age-related volumetric differences was the largest among the APOE ε4 carriers.

4 | DISCUSSION

This is the first in vivo study that examined the effects of healthy aging on the AG subnuclei. First, we found that volumes of the total AG, its BLA group, including the La, B, and AB nuclei showed significant nonlinear negative relationships with age, while the Co group demonstrated a trend towards significance. In contrast, the CeM group volume was not associated with age. Second, these age-related associations were found only in males, but not in females. We did not find any statistically significant effects of APOE and BDNF polymorphisms on the total AG and its subnuclei neither in younger or older adults. Nevertheless, both older APOE ε4 and ε3 allele carriers had smaller lateral, basal, and accessory basal nuclei volumes compared to their younger counterparts. In contrast, older and younger APOE ε2 allele carriers did not differ in their AG subnuclei volumes.

4.1 | Aging trajectory of the total AG

Previous in vivo structural MRI (Allen et al., 2005; Laakso et al., 1995; Malykhin et al., 2008; Mu et al., 1999; Murphy et al., 1996; Sublette et al., 2008) and postmortem (Heckers et al., 1990) studies reported a negative relationship between the AG volume and age, or smaller AG volumes in older compared to younger participants with volumetric reduction becoming more pronounced in advanced age (Grieve et al., 2011; Mu et al., 1999). In contrast, several other studies, including both in vivo MRI, (Jernigan et al., 2001; Pruessner et al., 2001) and postmortem (Brabec et al., 2010) did not observe any effects of age on the AG structure. Some of the discrepancies between our findings and the after-mentioned studies are likely driven by methodological differences. For instance, Pruessner et al. (2001) investigated the effects of age and sex on the AG and hippocampal volumes in individuals who were between 18 and 42 years old; however, no association between the AG volume and age was reported separately for men and women. In contrast, this study suggests that age-related volumetric reduction in the

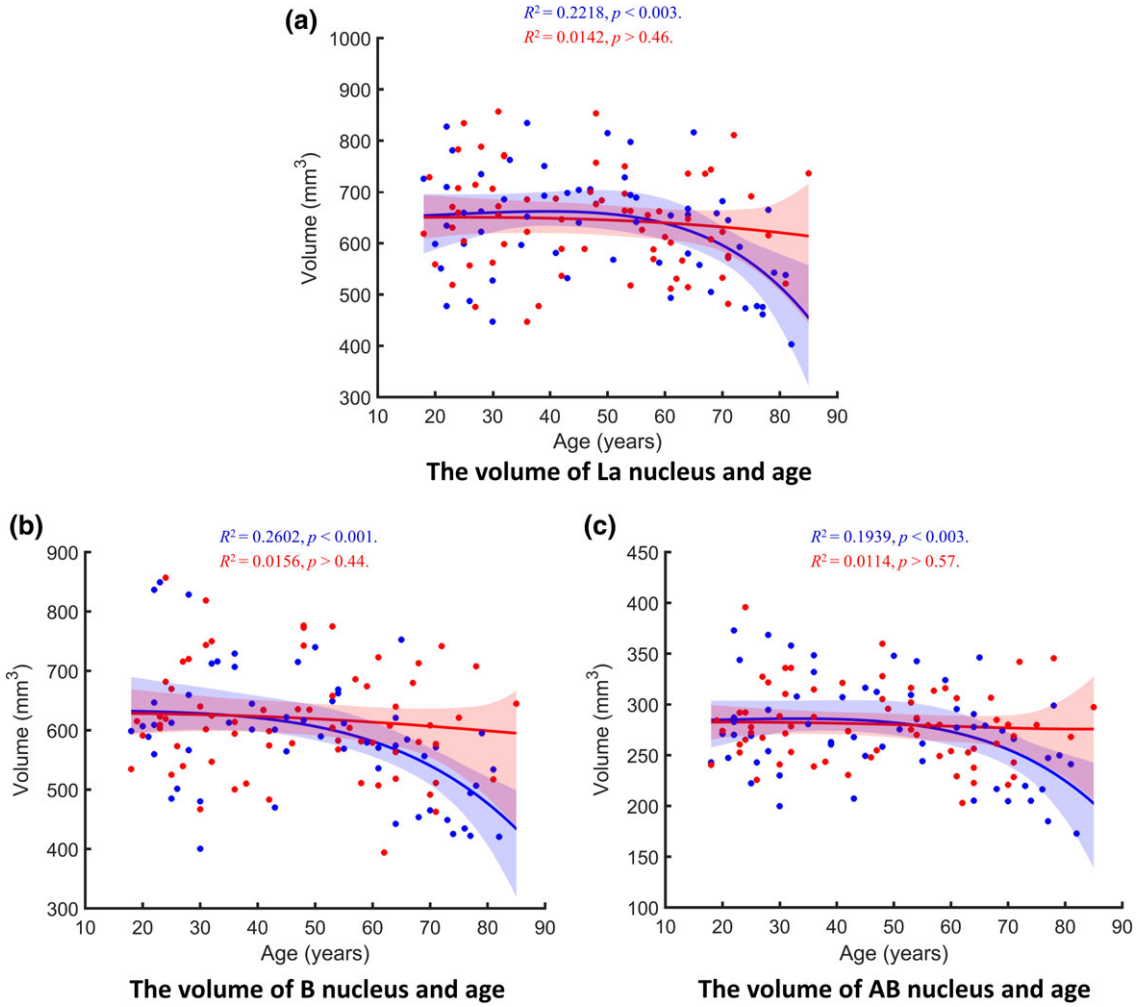

FIGURE 6 Regression plots showing the relationship between age and the ICV-adjusted volumes of BLA nuclei including (a) La, (b) B, and (c) AB. Model-averaged estimates for men (blue) and women (red) are shown separately. Shaded areas represent the 95% bootstrap percentile confidence interval for each fit. *P* values are corrected for multiple comparisons [Color figure can be viewed at wileyonlinelibrary.com]

AG starts in mid 50s. The most important difference between this study and Jernigan et al. (2001) is the definition of the AG boundary. Jernigan et al. (2001) combined the AG tissue with adjacent entorhinal and perirhinal cortices and used this "amygdala +" volume in their analysis, while in this study, these cortices were excluded from AG ROIs.

Although a published meta-analysis by Brierley et al. (2002) and a recent review article (Fjell & Walhovd, 2010) both suggested that the relationship between the AG volume and age is linear, our results demonstrated nonlinear correlations between age and volumes of the total AG and the AG subnuclei. Such inconsistencies could have arisen by infrequent use of nonlinear regression fits by other research groups: the majority of previous age-related MRI studies of the AG tested for linear correlations only (Brabec et al., 2010; Laakso et al., 1995; Mu et al., 1999; Pruessner et al., 2001; Sublette et al., 2008). A

TABLE 4 Summary of all regression models-related R^2, *p* values, and likelihood ratios (LR)

	Entire model[a]				Men				Women				Age × sex
ROIs	R^2	Prediction R^2	*p* value[b]	Nonlinearity LR	R^2	Prediction R^2	*p* value[b]	Nonlinearity LR	R^2	Prediction R^2	*p* value[b]	Nonlinearity LR	*p* value[b]
Total AG	.15	.06	<.002	71.90	.25	.13	<.001	55.44	.010	0	>.57	0.93	<.024
CeM	.03	0	>.480	2.24	.03	0	>.410	2.16	.005	0	>.66	1.08	>.233
Co	.08	0	<.092	15.75	.13	.03	<.021	10.86	.002	0	>.90	1.06	<.050
BLA	.16	.05	<.001	39.56	.26	.14	<.001	35.53	.017	0	>.40	0.91	<.030
La	.12	.01	<.006	65.77	.22	.12	<.003	75.85	.014	0	>.46	0.82	<.076
B	.16	.07	<.002	7.09	.26	.16	<.001	6.94	.016	0	>.44	0.99	<.024
AB	.12	.02	<.007	34.95	.19	.06	<.003	19.04	.010	0	>.57	1.05	<.035

[a] Entire regression model represents significance of at least one of the followings: main age effect, main sex effect, sex-specific age effect.
[b] *p* values are corrected for multiple comparisons.

TABLE 5 ICV-adjusted AG and its subnuclei volumes (mean ± SD) for the BDNF Met [Met+/+; Met+/−] and homozygous Val [+/+]) carriers

Alleles' frequency in the total sample					
Number of different BDNF genotypes carriers within the total sample (*n* = 126)					
	Met ≃ 0.19				**Val ≃ 0.81**
	Met/Met	**Met/Val**			**Val/Val**
Observed genotypes (*n*)[a]	4	39			83
Expected genotypes (*n*)[b]	4.55	38.78			82.67
Younger individuals (<55 years old)					
	BDNF phenotypes				
AG ROIs (mm^3)	**Met (*n* = 26)**	**Val (*n* = 51)**	***F* value**	***p* value**	**Effect size (Cohen's *d*)**
La	662.1 ± 88.96	653.22 ± 105.09	0.136	.71	0.091
B	643.92 ± 91.10	618.61 ± 96.23	1.234	.27	0.27
AB	284.91 ± 40.46	283.52 ± 40.12	0.021	.88	0.035
BLA	1,590.93 ± 190.52	1,555.35 ± 225.94	0.47	.49	0.17
Co	164.47 ± 21.28	164.93 ± 24.05	0.007	.93	0.02
CeM	303.14 ± 41.75	303.44 ± 49.95	0.001	.97	0.007
Total AG	2,058.54 ± 210.71	2,023.71 ± 262.15	0.345	.55	0.15
Older individuals (≥55 years old)					
	BDNF phenotypes				
AG ROIs (mm^3)	**Met (*n* = 17)**	**Val (*n* = 32)**	***F* value**	***p* value**	**Effect size (Cohen's *d*)**
La	623.58 ± 103.99	585.02 ± 82.78	2.01	.16	0.41
B	589.37 ± 92.27	544.50 ± 87.17	2.83	.09	0.50
AB	270.02 ± 42.56	254.86 ± 39.96	1.53	.22	0.37
BLA	1,482.96 ± 226.47	1,384.38 ± 188.51	2.64	.11	0.47
Co	160.58 ± 20.18	154.48 ± 27.48	0.65	.42	0.25
CeM	313.37 ± 37.9	293.83 ± 52.29	1.85	.18	0.43
Total AG	1,956.92 ± 270.29	1,832.7 ± 225.84	2.93	.09	0.50

[a] Observed genotypes represent the number of carriers for each genotype in the current sample.
[b] Expected genotypes represent the number of carriers for each genotype calculated using Met and Val frequencies.

few previous studies, which used a limited number of nonlinear regression models (Allen et al., 2005; Jernigan et al., 2001; Murphy et al., 1996), found no improvement in model fit by adding nonlinear terms to the model. However, two structural MRI studies, employing automated segmentation methods to estimate the AG volumes, showed that the rate of AG atrophy is not constant in advanced age (Fjell et al., 2009; Grieve et al., 2011). Therefore, future structural MRI studies of the relationship between the AG volume and age would need to test nonlinear models in addition to linear models to further address these discrepancies between studies.

It is important to mention that differences in MRI segmentation methods (e.g., manual vs automated) can lead to discrepancies in volumetric measures. Findings from studies that employed automated segmentation methods, such as the FreeSurfer and FSL-FIRST, need to be interpreted with caution because these software packages tend to overestimate both the AG and hippocampal volumes (Morey et al., 2009; Schoemaker et al., 2016). Discrepancies between manual segmentation and automated techniques are usually larger for the AG than for the hippocampal formation (Morey et al., 2009; Schoemaker et al., 2016). Furthermore, the accuracy of automatic segmentation methods might be further reduced in brains with noticeable atrophy (Sánchez-Benavides et al., 2010).

4.2 | Aging patterns of the AG subnuclei

Results of this study demonstrated a mosaic pattern of relationships between the AG subnuclei volumes and age. While the volumes of the La, B, and AB nuclei showed significant negative nonlinear associations with age, the CeM group did not correlate with age and the Co group showed a trend towards significance. The exact underlying reasons for the observed nonuniform correlations between the AG subnuclei volumes and age are not known. We speculate that these differences in vulnerability of the AG subnuclei to aging might be related to their heterogeneous connectivity profiles and function as well as evolutionarily features and developmental origins.

The number of the AG subnuclei varies from 13 subnuclei in rodents to 36 subnuclei in the humans (Yilmazer-Hanke, 2012). Each of the main AG subnuclei has specific functions through their unique anatomical connections (LeDoux, 2007).

The BLA group is connected to regions in the brain involved in learning and memory (Roozendaal, McEwen, & Chattarji, 2009) and these regions are vulnerable to the age-related changes (Fjell et al., 2013; Fjell & Walhovd, 2010; Jernigan et al., 2001; Looi & Sachdev, 2003; Malykhin et al., 2008; Malykhin et al., 2017; Raz & Kennedy, 2009; Walhovd et al., 2005). In contrast to the BLA, the CeM group is connected to the brain regions involved in regulation of autonomic

TABLE 6 ICV-adjusted AG and its subnuclei volumes (mean ± SD) for the APOE ε2 [ε2/x], homozygous ε3 [ε3/ε3], and ε4 [ε4/x]) carriers

Alleles' frequencies in the total sample						
Number of different APOE genotypes carriers within the total sample (*n* = 126)						
	ε2 ≃ 0.09			**ε3 ≃ 0.80**	**ε4 ≃ 0.11**	
	ε2/ε2	**ε2/ε3**	**ε2/ε4**	**ε3/ε3**	**ε3/ε4**	**ε4/ε4**
Observed genotypes (*n*)[a]	3	14	3	84	20	2
Expected genotypes (*n*)[b]	1.02	18.14	2.49	80.44	22.18	1.52

Younger individuals (<55 years old)						
	APOE phenotypes[c]					
AG ROIs (mm^3)	**ε2 (*n* = 11)**	**ε3 (*n* = 53)**	**ε4 (*n* = 13)**	***F* value**	***p* value**	**Effect size (η^2)**
La	624.54 ± 99.54	662.21 ± 100.64	658.60 ± 96.85	0.65	.52	.017
B	628.14 ± 84.96	629.22 ± 99.83	617.90 ± 86.50	0.07	.93	.002
AB	282.31 ± 30.35	284.60 ± 43.40	282.95 ± 34.41	0.02	.98	.001
BLA	1,534.99 ± 201.43	1,576.02 ± 222.71	1,559.44 ± 200.11	0.17	.84	.005
Co	167.49 ± 18.97	162.97 ± 24.50	169.84 ± 20.12	0.55	.58	.015
CeM	322.15 ± 26.79	295.10 ± 48.34	321.01 ± 48.36	2.73	.07[e]	.690
Total AG	2,024.64 ± 219.19	2,034.09 ± 259.02	2,050.29 ± 222.42	0.03	.97	.001

Older individuals (≥55 years old)						
	APOE phenotypes[c]					
AG ROIs (mm^3)	**ε2 (*n* = 6)**	**ε3 (*n* = 31)**	**ε4 (*n* = 9)**	***F* value**	***p* value**	**Effect size (η^2)**
La	662.01 ± 82.98	594.05 ± 93.03	560.69 ± 88.12	2.26	.12	.095
B	606.79 ± 71.97	558.55 ± 97.04	521.97 ± 82.82	1.54	.23	.067
AB	278.59 ± 37.76	258.25 ± 42.45	250.23 ± 44.93	0.86	.44	.037
BLA	1,547.39 ± 185.19	1,410.84 ± 215.6	1,332.89 ± 184.19	1.95	.16	.083
Co	169.89 ± 21.21	152.67 ± 27.40	158.04 ± 21.40	1.16	.32	.051
CeM	328.30 ± 21.04	292.08 ± 50.52	317.67 ± 50.64	2.04	.14	.087
Total AG	2,045.58 ± 213.41	1,855.59 ± 260.56	1,808.60 ± 227.16	1.81	.18	.078

Young vs Old[d]						
	ε2 (*n* = 17)		**ε3 (*n* = 84)**		**ε4 (*n* = 22)**	
AG ROIs (mm^3)	***p* value**	**Effect size (Cohen's *d*)**	***p* value**	**Effect size (Cohen's *d*)**	***p* value**	**Effect size (Cohen's *d*)**
La	.679	0.41	.005	0.70	.047	1.06
B	.762	0.27	.005	0.72	.039	1.13
AB	.826	0.11	.009	0.61	.067	0.82
BLA	.902	0.06	.004	0.75	.039	1.18
Co	.943	0.12	.013	0.40	.321	0.57
CeM	.923	0.26	.785	0.06	.880	0.07
Total AG	.850	0.10	.003	0.69	.022	1.08

[a] Observed genotypes represent the number of carriers for each genotype in the current sample.
[b] Expected genotypes represent the number of carriers for each genotype calculated using ε2, ε3, and ε4 frequencies.
[c] ε2/ε4 (*N* = 3) genotype was excluded from the volumetric analysis.
[d] All *p* values are corrected for multiple comparisons.
[e] A post hoc comparison, using the LSD test did not show any significant difference in the volume of the CeM group between APOE polymorphism carriers.

functions and mediating intrinsic behaviors (Roozendaal et al., 2009) which are resilient to age-related adversity (Doraiswamy et al., 1992; Fjell & Walhovd, 2010; Luft et al., 1999; Raz, 2000; Roberts, Killiany, & Rosene, 2012). Finally, age-related findings on the olfactory bulb which projects to the Co group remain inconsistent with both preservation and decrease in volume with age (Mobley, Rodriguez-Gil, Imamura, & Greer, 2014).

The second possible explanation for differential effects of aging processes on the AG subnuclei might be due to the ontogenetic (an individual's development) and phylogenetic (evolutionary history) properties of various brain regions (Raz et al., 1997). All the AG subnuclei can be categorized based on either their evolutionarily features (LeDoux, 2007; Swanson & Petrovich, 1998) or their developmental origins (Swanson & Petrovich, 1998; Yilmazer-Hanke, 2012).

According to phylogenetics, the AG is divided into two major groups: (1) the cortico-medial region including Co, medial (Me), and central (Ce) subnuclei which is a primitive division of the AG; and (2) the BLA group consisting of the La, B, and AB nuclei which is a phylogenetically newer division of the AG (LeDoux, 2007; Swanson & Petrovich, 1998). In this study, the CeM group was the only subregion in the AG that did not show any relationship with age. Chareyron, Banta Lavenex, Amaral, and Lavenex (2011) showed that the Me and

Ce nuclei comprise a conservative group that exhibited a relatively small size difference between rats and monkeys. In contrast, the BLA group (that showed significant negative correlations with age in this study) is noticeably more developed in monkeys and humans than in rats. While the BLA group comprises 62% and 69% of the total AG volume in monkeys and humans, respectively; it comprises only 28% of the total AG volume in rats (Chareyron et al., 2011). Therefore, it is likely that age-related susceptibility of the AG subnuclei might have phylogenetic underpinnings. In addition, the present finding on the preservation of the CeM group with age is consistent with the conservation of the autonomic AG [including Ce and Me nuclei that project to autonomically related structures in the brain (Roozendaal et al., 2009)] during evolution (Moreno & González, 2007). The CeM group is critically important in mediating behavioral responses to environmental stimuli (Moreno & González, 2007). Furthermore, a previous behavioral study showed that elderly adults have similar responses in detecting potentially threatening stimuli as young adults (Mather & Knight, 2006).

The AG subnuclei can also be categorized according to their developmental origins and preferential connections into three major groups: (1) the BLA group; (2) the superficial or Co-like group; and (3) the CeM group which includes the Ce and Me nuclei (Yilmazer-Hanke, 2012). The development of the AG subnuclei and their aging patterns may follow the notion that the last regions in the brain to mature are among the first to show the signs of aging (Raz et al., 1997; Raz et al., 2005).

Among the AG subnuclei, the Co and Me nuclei develop first (Humphrey, 1968). However, the Ce nucleus develops considerably later than the Co and Me nuclei. The BLA group also differentiates into its constituent nuclei much later than the Co and Me nuclei (Humphrey, 1968). Therefore, developmental patterns of the AG subnuclei might explain their aging patterns to some extent. Despite the developmental timing of the Co and Ce nuclei, the former showed a negative relationship with age and the latter did not correlate with age, which contrasts the "last in, first out" hypothesis (Fjell & Walhovd, 2010). It is important to mention that although we did not segment Ce and Me nuclei separately, due to the larger volume of the Ce compared to Me (almost two times) (García-Amado & Prensa, 2012); we think that if the Ce nucleus indeed underwent volumetric atrophy with age, the CeM group would also show such an effect.

In summary, in our view, heterogeneous connectivity profiles and phylogenetic properties of the AG subnuclei might play a more important role in their differential vulnerability to aging than their ontogenetic properties.

4.3 | Sexual dimorphism in the association of AG ROIs' volumes with age

In this study, we observed significant age × sex interactions in the total AG, the BLA, and Co groups, as well as the B and AB nuclei, while the La nucleus showed a trend towards significance for this interaction ($p < .076$).

The existence of a sex bias (Jazin & Cahill, 2010) in brain structures and functions as well as a healthy behavior across the lifespan has been previously suggested (Cosgrove, Mazure, & Staley, 2007; Gur, Bockow, & Gur, 2010; Jazin & Cahill, 2010). The effects of aging on the global gray matter volume and on other brain structures were previously compared between men and women (Abe et al., 2010; Coffey et al., 1998; Cowell et al., 1994; Good et al., 2001; Murphy et al., 1996; Raz et al., 2004) and only few brain structures showed greater volumetric reduction in women compared to men (Li et al., 2014; Murphy et al., 1996). In general, studies that reported age-specific differences between the two sexes, claimed that the effects of aging were more pronounced in men compared to women (Allen et al., 2005). It is important to note that, in contrast to the observed sex bias in aging patterns of the AG and its subnuclei, ICV-adjusted volumes of the AG and the AG subnuclei did not differ between men and women. This is in agreement with both postmortem (Brabec et al., 2010) and neuroimaging (Aghamohammadi-Sereshki et al., 2018; Giedd, Castellanos, Rajapakse, Vaituzis, & Rapoport, 1997; Karchemskiy et al., 2011; Laakso et al., 1995; Mu et al., 1999; Murphy et al., 1996; Pruessner et al., 2001; Sublette et al., 2008) studies. Although Brabec et al. (2010) did not find any associations between the AG volumes and age in both males and females, a negative correlation between age and a portion of the AG volume that represented the difference between the AG with wider borders ("$V_{Class+Add}$") (Brabec et al., 2010) and the classical definition of the AG ("V_{Class}") (Brabec et al., 2010) was reported in males, but not in females. In this study, the location and orientation of the AG subnuclei corresponded to the classical definition of the AG ("V_{Class}") (Brabec et al., 2010). However, due to lack of visible landmarks on MRI for delineation of the anterior AG from the periamygdaloid cortices (Aghamohammadi-Sereshki et al., 2018; Allen et al., 2005), inclusion of some of the "V_{add}" (Brabec et al., 2010) tissue in our AG subnuclei segmentation method was inevitable. Therefore, our findings on age-related sexual dimorphism are partially in agreement with Brabec et al. (2010). Moreover, Giedd et al. (1997) reported sex differences in the AG maturation among 115 healthy children and adolescents with greater age-related volumetric increase in males than in females (Giedd et al., 1997).

The etiology of sexual dimorphism in neuroscience is not clear for two main reasons: first, the widespread use of male animals in preclinical studies; and second, a false conception that considers sex bias as minor and unimportant (Cahill & Aswad, 2015).

In general, the most plausible explanations for sexual differences are (1) estrogen and androgen-dependent mechanisms (Behl, 2002; Cosgrove et al., 2007) and (2) sexual regulatory mechanisms independent of sexual hormones (Cahill, 2006; Jazin & Cahill, 2010). Sex hormones have considerable effect on the AG (Hamann, Herman, Nolan, & Wallen, 2004). In human and nonhuman primate AG, the Ce nucleus is the only major nucleus without any report of estrogen receptor alpha (ERα)-immunoreactive neurons, mRNA expression of ERα and estrogen receptor beta (ERβ) in both sexes; and also, without any report of cytochrome P450 aromatase and androgen receptor mRNA expressions in males (Blurton-Jones et al., 1999; Österlund, Gustafsson, et al., 2000a, 2000b; Roselli et al., 2001). However, these sexual hormones markers are differentially distributed in the rest of the AG subnuclei (Blurton-Jones et al., 1999; Österlund, Gustafsson, et al., 2000a, 2000b; Roselli et al., 2001). Age-related decrease of the ERβ mRNA expression was reported in the B nucleus and nucleus of the lateral olfactory tract [a part of the Co group (Sah et al., 2003)] of

female rats (Yamaguchi-Shima & Yuri, 2007), while the La, anterior and posterior cortical, and Ce nuclei showed reduced ERβ mRNA expression in male rats (Yamaguchi & Yuri, 2012), suggesting that these effects were sex-dependent (Yamaguchi & Yuri, 2012).

Estrogen can also enhance neuron longevity via its neurotrophic and antioxidant roles or by suppressing apoptosis (Behl, 2002). Future studies will need to determine neuroprotective effects of estrogen on human AG in aging.

4.4 | Imaging genetics of the AG

In this study, we did not find any statistically significant effect of the BDNF and APOE polymorphisms on the AG and its subnuclei volumes.

The main objective of neuroimaging genetics is to identify genes that either precipitate or lessen deleterious age-related effects on brain structures and their functions (Fjell & Walhovd, 2010). Although lipoprotein transport and neuronal health are the two primary functions of APOE in the brain (Petrella et al., 2008), structural effects of APOE on brain regions are still poorly understood in healthy populations (Fjell & Walhovd, 2010). Most of the APOE studies have focused on the hippocampus, though findings are contradictory. While some studies found negative effects of APOE ε4 alleles on the hippocampal volumes in the elderly, other studies did not report hippocampal volume differences between healthy APOE ε4 carriers versus noncarriers in nondemented older adults (Fjell & Walhovd, 2010). However, data about the AG and APOE genetic polymorphisms in healthy aging is scarce. One study, which used a manual segmentation procedure on 428 nondemented elderly individuals found that carriers of ε4 had significantly smaller bilateral AG than ε3ε3 genotype carriers. Furthermore, although ε2 carriers had more atrophy than those with the ε3ε3 genotype, the difference was not significant (den Heijer et al., 2002). A large neuroimaging-genetics study (30,717 individuals from 50 cohorts), which used automated segmentation tools (FSL-FIRST and FreeSurfer) did not find any association between the AG volume with either APOE or BDNF, and the AG showed the least heritability (h^2 = 0.43; confidence interval = 0.39, 0.48) among all the examined subcortical regions (Hibar et al., 2015). Finally, Soldan et al. (2015) demonstrated that the AG volume estimated using a semi-automated technique (n = 245) did not depend on APOE-ε4 genotype.

BDNF is the most abundant neuronal growth factor (Sublette et al., 2008) which plays a key role in neuronal survival, synaptogenesis, proliferation, and development (Petrella et al., 2008). Several studies showed that Val66Met genotype is associated with decreased volume in the hippocampus, prefrontal cortex, and temporal and occipital gray matter (Petrella et al., 2008; Sublette et al., 2008). Like APOE, the relationship between BDNF and AG has been less studied. In addition to Hibar et al. (2015), Sublette et al. (2008) explored the relationship between age, BDNF, and AG volumes among 55 healthy right-handed volunteers using a manual tracing procedure. They found no difference in the raw and ICV-adjusted bilateral AG volumes between BDNF val66met allele carriers and noncarriers and reported an inverse correlation between the AG volume and age in BDNF val66met carriers but not in noncarriers. However, the authors suggested that these results should be interpreted with caution due to the small sample size, limited age range, and inadequate statistical power to detect sex differences (Sublette et al., 2008).

Our findings are consistent with previous results reported by Hibar et al. (2015) and Sublette et al. (2008), which reported absence of a relationship between the AG volume and APOE or BDNF polymorphisms. Our results are also in partial agreement with those by Soldan et al. (2015) who demonstrated that the AG volume did not differ between APOE-ε4 carriers and noncarriers. However, this study differs from previous research by den Heijer et al. (2002), which indicated ε4 carriers have more AG atrophy than ε3ε3 carriers.

Our result on relative preservation of AG subnuclei in ε2 carriers versus ε4 is in line with previous research, which indicated that the APOE ε2 allele can reduce the risk of developing Alzheimer's disease as it has positive survival and longevity effects in elderly individuals (Corder et al., 1996; Schächter et al., 1994; Wisdom et al., 2011), while homozygous APOE ε4 allele carriers are 10–12 times more likely to develop the late-onset Alzheimer's disease (Farrer et al., 1997). However, volumes of the AG subnuclei in ε2 carriers were not statistically different form participants with the most common ε3 variant of APOE that is not associated with Alzheimer's disease (Corder et al., 1996; Lahiri, Sambamurti, & Bennett, 2004; Wisdom et al., 2011). Although, in this study ε3 carriers did not differ in any AG subnuclei volumes from ε4 carriers, and age-related decline in AG volume was found in both groups, the larger effect size of AG volume decline with age in ε4 carriers could indicate that cognitively healthy participants with APOE ε4 allele were more vulnerable to aging than ε3 carriers and especially more than ε2 carriers. As our sample size of ε2 and ε4 carriers in aging subgroups was relatively small, future studies with substantially larger samples are needed to provide a conclusive evidence of neuroprotective effect of ε2 on the AG subnuclei.

It is important to mention that gene × environment interactions might also obscure effects of a specific gene on individual brain structures (Fjell & Walhovd, 2010). Finally, considerable differences in gene expression of various age cohorts (e.g., old vs young adults) further challenge our ability to detect the effect a single gene might have on each individual brain structure (Reinvang et al., 2010).

5 | LIMITATIONS AND FUTURE DIRECTIONS

This study was cross-sectional and therefore future longitudinal studies would have to address the nature and rate of the AG volume loss in healthy aging. Modest sample size for the genetic component of our study, particularly the number of ε2 carriers, could have prevented us from detecting any significant protective effects of this allele against aging. However, larger neuroimaging genetic studies might require the application of automated segmentation methods which might reduce the segmentation accuracy of the medial temporal lobe structures. The current manual segmentation protocol of the AG subnuclei is based on geometrical rules dependant on internal AG landmarks as the AG myelinated fibers are not visible even at 4.7 T FSE images (Aghamohammadi-Sereshki et al., 2018). Therefore, our macroscopically defined AG subnuclei are only an approximation of the individual microscopical subnuclei. Despite the fact that 4.7 T system is

quite rare, similar high-resolution MRI protocols have been successfully employed in aging studies of hippocampal subfields that used both lower (3 T) and higher (7 T) field strength magnets (see Malykhin et al., 2017). Future volumetric MRI studies would also need to determine whether the reported differences in aging patterns between the AG subnuclei are associated with differences in cognitive or affective functions.

ACKNOWLEDGMENTS

Financial support for this study was provided by the Canadian Institutes of Health Research (CIHR) operating grant MOP115011 to Nikolai Malykhin. Scott Travis was supported by the CIHR Frederick Banting and Charles Best Canada Masters scholarship award and the Alberta Innovates Health Solutions (AIHS) Doctoral scholarship award. Stanislau Hrybouski was supported by Fredrick Banting and Charles Best CIHR Doctoral scholarship award. We would like to thank members of the Applied Genomics Core (TAGC, Faculty of Medicine & Dentistry, University of Alberta), Dr. Andrew L. Mason (Director), Dr. Georgina Macintyre and Ms Susan Kenney for their help with genetic data collection. The authors have no conflicts of interest to disclose.

ORCID

Nikolai V. Malykhin https://orcid.org/0000-0002-7691-5050

REFERENCES

Abe, O., Yamasue, H., Yamada, H., Masutani, Y., Kabasawa, H., Sasaki, H., … Ohtomo, K. (2010). Sex dimorphism in gray/white matter volume and diffusion tensor during normal aging. *NMR in Biomedicine*, *23*, 446–458.

Adolphs, R. (2009). The social brain: Neural basis of social knowledge. *Annual Review of Psychology*, *60*, 693–716.

Aghamohammadi-Sereshki, A., Huang, Y., Olsen, F., & Malykhin, N. V. (2018). In vivo quantification of amygdala subnuclei using 4.7 T fast spin echo imaging. *NeuroImage*, *170*, 151–163. https://doi.org/10.1016/j.neuroimage

Allen, J. S., Bruss, J., Brown, C. K., & Damasio, H. (2005). Normal neuroanatomical variation due to age: The major lobes and a parcellation of the temporal region. *Neurobiology of Aging*, *26*, 1245–1260 discussion 1279-1282.

Basso, M., Gelernter, J., Yang, J., MacAvoy, M. G., Varma, P., Bronen, R. A., & van Dyck, C. H. (2006). Apolipoprotein E epsilon4 is associated with atrophy of the amygdala in Alzheimer's disease. *Neurobiology of Aging*, *2710*, 1416–1424.

Behl, C. (2002). Oestrogen as a neuroprotective hormone. *Nature Reviews. Neuroscience*, *3*, 433–442.

Blurton-Jones, M. M., Roberts, J. A., & Tuszynski, M. H. (1999). Estrogen receptor immunoreactivity in the adult primate brain: Neuronal distribution and association with p75, trkA, and choline acetyltransferase. *Journal of Comparative Neurology*, *405*, 529–542.

Bonilha, L., Kobayashi, E., Cendes, F., & Min Li, L. (2004). Protocol for volumetric segmentation of medial temporal structures using high-resolution 3-D magnetic resonance imaging. *Human Brain Mapping*, *22*, 145–154.

Braak, H., Braak, E., Yilmazer, D., de Vos, R. A., Jansen, E. N., Bohl, J., & Jellinger, K. (1994). Amygdala pathology in Parkinson's disease. *Acta Neuropathologica*, *88*, 493–500.

Brabec, J., Rulseh, A., Hoyt, B., Vizek, M., Horinek, D., Hort, J., & Petrovicky, P. (2010). Volumetry of the human amygdala—An anatomical study. *Psychiatry Research*, *182*, 67–72.

Brierley, B., Shaw, P., & David, A. S. (2002). The human amygdala: A systematic review and meta-analysis of volumetric magnetic resonance imaging. *Brain Research. Brain Research Reviews*, *39*, 84–105.

Brown, T. A., Di Nardo, P. A., Lehman, C. L., & Campbell, L. A. (2001). Reliability of DSM-IV anxiety and mood disorders: Implications for the classification of emotional disorders. *Journal of Abnormal Psychology*, *110*, 49–58.

Burnham, K. P., & Anderson, D. R. (2002). *Model selection and multimodel inference: A practical information-theoretic approach* (2nd ed.). New York: Springer-Verlag.

Cahill, L. (2006). Why sex matters for neuroscience. *Nature Reviews. Neuroscience*, *7*, 477–484.

Cahill, L., & Aswad, D. (2015). Sex influences on the brain: An issue whose time has come. *Neuron*, *88*, 1084–1085.

Casey, G. (2013). Parkinson's disease: A long and difficult journey. *Nursing New Zealand*, *19*, 20–24.

Chareyron, L. J., Banta Lavenex, P., Amaral, D. G., & Lavenex, P. (2011). Stereological analysis of the rat and monkey amygdala. *Journal of Comparative Neurology*, *519*, 3218–3239.

Coffey, C. E., Lucke, J. F., Saxton, J. A., Ratcliff, G., Unitas, L. J., Billig, B., & Bryan, R. N. (1998). Sex differences in brain aging: A quantitative magnetic resonance imaging study. *Archives of Neurology*, *55*, 169–179.

Corder, E. H., Lannfelt, L., Viitanen, M., Corder, L. S., Manton, K. G., Winblad, B., & Basun, H. (1996). Apolipoprotein E genotype determines survival in the oldest old (85 years or older) who have good cognition. *Archives of Neurology*, *53*, 418–422.

Cosgrove, K. P., Mazure, C. M., & Staley, J. K. (2007). Evolving knowledge of sex differences in brain structure, function, and chemistry. *Biological Psychiatry*, *62*, 847–855.

Cowell, P. E., Turetsky, B. I., Gur, R. C., Grossman, R. I., Shtasel, D. L., & Gur, R. E. (1994). Sex differences in aging of the human frontal and temporal lobes. *The Journal of Neuroscience*, *14*, 4748–4755.

Deary, I. J., Wright, A. F., Harris, S. E., Whalley, L. J., & Starr, J. M. (2004). Searching for genetic influences on normal cognitive ageing. *Trends in Cognitive Sciences*, *8*, 178–184.

den Heijer, T., Oudkerk, M., Launer, L. J., van Duijn, C. M., Hofman, A., & Breteler, M. M. (2002). Hippocampal, amygdalar, and global brain atrophy in different apolipoprotein E genotypes. *Neurology*, *59*, 746–748.

Doraiswamy, P. M., Na, C., Husain, M. M., Figiel, G. S., McDonald, W. M., Ellinwood, E. H., Jr., … Krishnan, K. R. (1992). Morphometric changes of the human midbrain with normal aging: MR and stereologic findings. *AJNR. American Journal of Neuroradiology*, *13*, 383–386.

Duyn, J. H. (2012). The future of ultra-high field MRI and fMRI for study of the human brain. *NeuroImage*, *62*, 1241–1248.

Efron, B., & Tibshirani, R. (1997). Improvements on cross-validation: The .632+ bootstrap method. *Journal of the American Statistical Association*, *92*, 548–560.

Entis, J. J., Doerga, P., Barrett, L. F., & Dickerson, B. C. (2012). A reliable protocol for the manual segmentation of the human amygdala and its subregions using ultra-high resolution MRI. *NeuroImage*, *60*, 1226–1235.

Farrer, L. A., Cupples, L. A., Haines, J. L., Hyman, B., Kukull, W. A., Mayeux, R., … van Duijn, C. M. (1997). Effects of age, sex, and ethnicity on the association between apolipoprotein E genotype and Alzheimer disease. A meta analysis. APOE and Alzheimer Disease Meta Analysis Consortiume. *JAMA*, *278*, 1349–1356.

Fjell, A. M., & Walhovd, K. B. (2010). Structural brain changes in aging: Courses, causes and cognitive consequences. *Reviews in the Neurosciences*, *21*, 187–221.

Fjell, A. M., Westlye, L. T., Amlien, I., Espeseth, T., Reinvang, I., Raz, N., … Walhovd, K. B. (2009). Minute effects of sex on the aging brain: A multisample magnetic resonance imaging study of healthy aging and Alzheimer's disease. *The Journal of Neuroscience*, *29*, 8774–8783.

Fjell, A. M., Westlye, L. T., Grydeland, H., Amlien, I., Espeseth, T., Reinvang, I., … Alzheimer Disease Neuroimaging Initiative. (2013). Critical ages in the life course of the adult brain: Nonlinear subcortical aging. *Neurobiology of Aging*, *34*, 2239–2247.

Freese, J. L., & Amaral, D. G. (2009). Neuroanatomy of the primate amygdala. In P. J. Whalen & E. A. Phelps (Eds.), *The human amygdala* (pp. 3–42). New York: The Guilford Press.

Galvin, J. E., Roe, C. M., Coats, M. A., & Morris, J. C. (2007). Patient's rating of cognitive ability: Using the AD8, a brief informant interview, as a self-rating tool to detect dementia. *Archives of Neurology*, *64*, 725–730.

García-Amado, M., & Prensa, L. (2012). Stereological analysis of neuron, glial and endothelial cell numbers in the human amygdaloid complex. *PLoS One*, *7*(6), e38692.

Giedd, J. N., Castellanos, F. X., Rajapakse, J. C., Vaituzis, A. C., & Rapoport, J. L. (1997). Sexual dimorphism of the developing human brain. *Progress in Neuro-Psychopharmacology & Biological Psychiatry*, *21*, 1185–1201.

Good, C. D., Johnsrude, I. S., Ashburner, J., Henson, R. N., Friston, K. J., & Frackowiak, R. S. (2001). A voxel-based morphometric study of ageing in 465 normal adult human brains. *NeuroImage*, *14*, 21–36.

Grieve, S. M., Korgaonkar, M. S., Clark, C. R., & Williams, L. M. (2011). Regional heterogeneity in limbic maturational changes: Evidence from integrating cortical thickness, volumetric and diffusion tensor imaging measures. *NeuroImage*, *55*, 868–879.

Gur, R. C., Bockow, T., & Gur, R. E. (2010). Gender differences in the functional organization of the brain. In M. J. Legato (Ed.), *Principles of gender-specific medicine* (2nd ed., pp. 75–86). San Diego: Elsevier Academic Press.

Hachinski, V. C., Iliff, L. D., Zilhka, E., Du Boulay, G. H., McAllister, V. L., Marshall, J., … Symon, L. (1975). Cerebral blood flow in dementia. *Archives of Neurology*, *32*, 632–637.

Hamann, S., Herman, R. A., Nolan, C. L., & Wallen, K. (2004). Men and women differ in amygdala response to visual sexual stimuli. *Nature Neuroscience*, *7*, 411–416.

Hampton, A. N., Adolphs, R., Tyszka, M. J., & O'Doherty, J. P. (2007). Contributions of the amygdala to reward expectancy and choice signals in human prefrontal cortex. *Neuron*, *55*, 545–555.

Harding, A. J., Stimson, E., Henderson, J. M., & Halliday, G. M. (2002). Clinical correlates of selective pathology in the amygdala of patients with Parkinson's disease. *Brain*, *125*(Pt 11), 2431–2445.

Hashimoto, M., Yasuda, M., Tanimukai, S., Matsui, M., Hirono, N., Kazui, H., & Mori, E. (2001). Apolipoprotein E epsilon 4 and the pattern of regional brain atrophy in Alzheimer's disease. *Neurology*, *57*, 1461–1466.

Heckers, S., Heinsen, H., Heinsen, Y. C., & Beckmann, H. (1990). Limbic structures and lateral ventricle in schizophrenia. A quantitative post-mortem study. *Archives of General Psychiatry*, *47*, 1016–1022.

Hesterberg, T., Moore, D. S., Monagham, S., Clipson, A., & Epstein, R. (2009). Bootstrap methods and permutation tests. In D. S. Moore, M. C. GP, & B. A. Craig (Eds.), *Introduction to the practice of statistics* (6th ed., pp. 16_1–16_60). New York: W.H. Freeman.

Hibar, D. P., Stein, J. L., Renteria, M. E., Arias-Vasquez, A., Desrivières, S., Jahanshad, N., … Medland, S. E. (2015). Common genetic variants influence human subcortical brain structures. *Nature*, *520*, 224–229.

Honea, R. A., Vidoni, E., Harsha, A., & Burns, J. M. (2009). Impact of APOE on the healthy aging brain: A voxel-based MRI and DTI study. *Journal of Alzheimer's Disease*, *18*, 553–564.

Hughes, C. P., Berg, L., Danziger, W. L., Coben, L. A., & Martin, R. L. (1982). A new clinical scale for the staging of dementia. *The British Journal of Psychiatry*, *140*, 566–572.

Humphrey, T. (1968). The development of the human amygdala during early embryonic life. *Journal of Comparative Neurology*, *132*, 135–165.

Jazin, E., & Cahill, L. (2010). Sex differences in molecular neuroscience: From fruit flies to humans. *Nature Reviews. Neuroscience*, *11*, 9–17.

Jernigan, T. L., Archibald, S. L., Fennema-Notestine, C., Gamst, A. C., Stout, J. C., Bonner, J., & Hesselink, J. R. (2001). Effects of age on tissues and regions of the cerebrum and cerebellum. *Neurobiology of Aging*, *22*, 581–594.

Karchemskiy, A., Garrett, A., Howe, M., Adleman, N., Simeonova, D. I., Alegria, D., … Chang, K. (2011). Amygdalar, hippocampal, and thalamic volumes in youth at high risk for development of bipolar disorder. *Psychiatry Research*, *194*, 319–325.

Krasuski, J. S., Alexander, G. E., Horwitz, B., Daly, E. M., Murphy, D. G., Rapoport, S. I., & Schapiro, M. B. (1998). Volumes of medial temporal lobe structures in patients with Alzheimer's disease and mild cognitive impairment (and in healthy controls). *Biological Psychiatry*, *43*(1), 60–68.

Laakso, M. P., Partanen, K., Lehtovirta, M., Hallikainen, M., Hänninen, T., Vainio, P., … Soininen, H. (1995). MRI of amygdala fails to diagnose early Alzheimer's disease. *NeuroReport*, *6*, 2414–2418.

Lahiri, D. K., Sambamurti, K., & Bennett, D. A. (2004). Apolipoprotein gene and its interaction with the environmentally driven risk factors: Molecular, genetic and epidemiological studies of Alzheimer's disease. *Neurobiology of Aging*, *25*, 651–660.

LeDoux, J. (2007). The amygdala. *Current Biology*, *17*, R868–R874.

LeDoux, J. E., & Schiller, D. (2009). The human amygdala insight from other animals. In P. J. Whalen & E. A. Phelps (Eds.), *The human amygdala* (pp. 43–60). New York: The Guilford Press.

Li, W., van Tol, M. J., Li, M., Miao, W., Jiao, Y., Heinze, H. J., … Walter, M. (2014). Regional specificity of sex effects on subcortical volumes across the lifespan in healthy aging. *Human Brain Mapping*, *35*, 238–247.

Looi, J. C. L., & Sachdev, P. S. (2003). Structural neuroimaging of the ageing brain. In P. S. Sachdev (Ed.), *The ageing brain: The neurobiology and neuropsychiatry of ageing* (pp. 49–63). Netherlands: Swets & Zeitlinger Publishers.

Luft, A. R., Skalej, M., Schulz, J. B., Welte, D., Kolb, R., Bürk, K., … Voight, K. (1999). Patterns of age-related shrinkage in cerebellum and brainstem observed in vivo using three-dimensional MRI volumetry. *Cerebral Cortex*, *9*, 712–721.

Mai, J. K., Paxinos, G., & Voss, T. (2008). *Atlas of the human brain* (third ed., pp. 135–167). New York: Elsevier Academic Press.

Malykhin, N. V., Bouchard, T. P., Camicioli, R., & Coupland, N. J. (2008). Aging hippocampus and amygdala. *NeuroReport*, *19*, 543–547.

Malykhin, N. V., Bouchard, T. P., Ogilvie, C. J., Coupland, N. J., Seres, P., & Camicioli, R. (2007). Three-dimensional volumetric analysis and reconstruction of amygdala and hippocampal head, body and tail. *Psychiatry Research: Neuroimaging*, *155*, 155–165.

Malykhin, N. V., Huang, Y., Hrybouski, S., & Olsen, F. (2017). Differential vulnerability of hippocampal subfields and anteroposterior hippocampal subregions in healthy cognitive aging. *Neurobiology of Aging*, *59*, 121–134.

Mankiw, C., Park, M. T. M., reardon, P. K., Fish, A. M., Clasen, L. S., Greenstein, D., … Raznahan, A. (2017). Allometric analysis detects brain size-independent effects of sex and sex chromosome complement on human cerebellar organization. *The Journal of Neuroscience*, *37*, 5221–5231.

Mather, M. (2016). The affective neuroscience of aging. *Annual Review of Psychology*, *67*, 213–238.

Mather, M., & Knight, M. R. (2006). Angry faces get noticed quickly: Threat detection is not impaired among older adults. *The Journals of Gerontology. Series B, Psychological Sciences and Social Sciences*, *61*, 54–57.

Matsuoka, Y., Mori, E., Inagaki, M., Kozaki, Y., Nakano, T., Wenner, M., & Uchitomi, Y. (2003). Manual tracing guideline for volumetry of hippocampus and amygdala with high-resolution MRI. *Nō to Shinkei*, *55*, 690–697.

Michielse, S., Coupland, N., Camicioli, R., Carter, R., Seres, P., Sabino, J., & Malykhin, N. (2010). Selective effects of aging on brain white matter microstructure: A diffusion tensor imaging tractography study. *NeuroImage*, *52*, 1190–1201.

Mobley, A. S., Rodriguez-Gil, D. J., Imamura, F., & Greer, C. A. (2014). Aging in the olfactory system. *Trends in Neurosciences*, *37*, 77–84.

Moore, D. S., McCabe, G. P., & Craig, B. A. (2009). *Introduction to the practice of statistics* (6th ed., pp. 607–636). New York: W.H. Freeman.

Moreno, N., & González, A. (2007). Evolution of the amygdaloid complex in vertebrates, with special reference to the anamnio-amniotic transition. *Journal of Anatomy*, *211*, 151–163.

Morey, R. A., Petty, C. M., Xu, Y., Hayes, J. P., Wagner, H. R. 2nd., Lewis, D. V., … McCarthy, G. (2009). A comparison of automated segmentation and manual tracing for quantifying hippocampal and amygdala volumes. *NeuroImage*, *45*, 855–866.

Moroney, J. T., Bagiella, E., Desmond, D. W., Hachinski, V. C., Mölsä, P. K., Gustafson, L., … Tatemichi, T. K. (1997). Meta-analysis of the Hachinski ischemic score in pathologically verified dementias. *Neurology*, *49*, 1096–1105.

Mu, Q., Xie, J., Wen, Z., Weng, Y., & Shuyun, Z. (1999). A quantitative MR study of the hippocampal formation, the amygdala, and the temporal

horn of the lateral ventricle in healthy subjects 40 to 90 years of age. *AJNR. American Journal of Neuroradiology*, *20*, 207–211.

Murphy, D. G., DeCarli, C., McIntosh, A. R., Daly, E., Mentis, M. J., Pietrini, P., … Rapoport, S. I. (1996). Sex differences in human brain morphometry and metabolism: An in vivo quantitative magnetic resonance imaging and positron emission tomography study on the effect of aging. *Archives of General Psychiatry*, *53*, 585–594.

Nasreddine, Z. S., Phillips, N. A., Bédirian, V., Charbonneau, S., Whitehead, V., Collin, I., … Chertkow, H. (2005). The Montreal cognitive assessment, MoCA: A brief screening tool for mild cognitive impairment. *Journal of the American Geriatrics Society*, *53*, 695–699.

Nordenskjöld, R., Malmberg, F., Larsson, E. M., Simmons, A., Ahlström, H., Johansson, L., & Kullberg, J. (2015). Intracranial volume normalization methods: Considerations when investigating gender differences in regional brain volume. *Psychiatry Research*, *231*, 227–235.

Oldfield, R. C. (1971). The assessment and analysis of handedness: The Edinburgh inventory. *Neuropsychologia*, *9*, 97–113.

Österlund, M. K., Gustafsson, J. A., Keller, E., & Hurd, Y. L. (2000a). Estrogen receptor beta (ERbeta) messenger ribonucleic acid (mRNA) expression within the human forebrain: Distinct distribution pattern to ERalpha mRNA. *The Journal of Clinical Endocrinology and Metabolism*, *85*, 3840–3846.

Österlund, M. K., Keller, E., & Hurd, Y. L. (2000b). The human forebrain has discrete estrogen receptor alpha messenger RNA expression: High levels in the amygdaloid complex. *Neuroscience*, *95*, 333–342.

Petrella, J. R., Mattay, V. S., & Doraiswamy, P. M. (2008). Imaging genetics of brain longevity and mental wellness: The next frontier? *Radiology*, *246*, 20–32.

Pruessner, J. C., Collins, D. L., Pruessner, M., & Evans, A. C. (2001). Age and gender predict volume decline in the anterior and posterior hippocampus in early adulthood. *The Journal of Neuroscience*, *21*, 194–200.

Raz, N. (2000). Aging of the brain and its impact on cognitive performance: Integration of structural and functional findings. In F. I. M. Craik & T. A. Salthouse (Eds.), *The handbook of aging and cognition* (2nd ed., pp. 1–90). Mahwah, NJ: Lawrence Erlbaum Associates.

Raz, N., Ghisletta, P., Rodrigue, K. M., Kennedy, K. M., & Lindenberger, U. (2010). Trajectories of brain aging in middle-aged and older adults: Regional and individual differences. *NeuroImage*, *51*, 501–511.

Raz, N., Gunning, F. M., Head, D., Dupuis, J. H., McQuain, J., Briggs, S. D., … Acker, J. D. (1997). Selective aging of the human cerebral cortex observed in vivo: Differential vulnerability of the prefrontal gray matter. *Cerebral Cortex*, *7*, 268–282.

Raz, N., Gunning-Dixon, F., Head, D., Rodrigue, K. M., Williamson, A., & Acker, J. D. (2004). Aging, sexual dimorphism, and hemispheric asymmetry of the cerebral cortex: Replicability of regional differences in volume. *Neurobiology of Aging*, *25*, 377–396.

Raz, N., & Kennedy, K. M. (2009). A systems approach to the aging brain: Neuroanatomic changes, their modifiers, and cognitive correlates. In W. Jagust & M. D'Esposito (Eds.), *Imaging the aging brain* (pp. 43–70). New York: Oxford University Press.

Raz, N., Lindenberger, U., Rodrigue, K. M., Kennedy, K. M., Head, D., Williamson, A., … Acker, J. D. (2005). Regional brain changes in aging healthy adults: General trends, individual differences and modifiers. *Cerebral Cortex*, *11*, 1676–1689.

Raz, N., & Rodrigue, K. M. (2006). Differential aging of the brain: Patterns, cognitive correlates and modifiers. *Neuroscience and Biobehavioral Reviews*, *30*, 730–748.

Reardon, P. K., Clasen, L., Giedd, J. N., Blumenthal, J., Lerch, J. P., Chakravarty, M. M., & Raznahan, A. (2016). An Allometric analysis of sex and sex chromosome dosage effects on subcortical anatomy in humans. *The Journal of Neuroscience*, *36*, 2438–2448.

Reiman, E. M., Caselli, R. J., Yun, L. S., Chen, K., Bandy, D., Minoshima, S., … Osborne, D. (1996). Preclinical evidence of Alzheimer's disease in persons homozygous for the epsilon 4 allele for apolipoprotein E. *The New England Journal of Medicine*, *334*, 752–758.

Reiman, E. M., Chen, K., Alexander, G. E., Caselli, R. J., Bandy, D., Osborne, D., … Hardy, J. (2004). Functional brain abnormalities in young adults at genetic risk for late-onset Alzheimer's dementia. *Proceedings of the National Academy of Sciences of the United States of America*, *101*, 284–289.

Reinvang, I., Deary, I. J., Fjel, A. M., Steen, V. M., Espeseth, T., & Parasuraman, R. (2010). Neurogenetic effects on cognition in aging brains: A window of opportunity for intervention? *Frontiers in Aging Neuroscience*, *2*, 1–15.

Roberts, D. E., Killiany, R. J., & Rosene, D. L. (2012). Neuron numbers in the hypothalamus of the normal aging rhesus monkey: Stability across the adult lifespan and between the sexes. *Journal of Comparative Neurology*, *520*, 1181–1197.

Roozendaal, B., McEwen, B. S., & Chattarji, S. (2009). Stress, memory and the amygdala. *Nature Reviews. Neuroscience*, *10*, 423–433.

Roselli, C. E., Klosterman, S., & Resko, J. A. (2001). Anatomic relationships between aromatase and androgen receptor mRNA expression in the hypothalamus and amygdala of adult male cynomolgus monkeys. *Journal of Comparative Neurology*, *439*, 208–223.

Sah, P., Faber, E. S., Lopez De Armentia, M., & Power, J. (2003). The amygdaloid complex: Anatomy and physiology. *Physiological Reviews*, *83*, 803–834.

Sánchez-Benavides, G., Gómez-Ansón, B., Sainz, A., Vives, Y., Delfino, M., & Peña-Casanova, J. (2010). Manual validation of FreeSurfer's automated hippocampal segmentation in normal aging, mild cognitive impairment, and Alzheimer disease subjects. *Psychiatry Research*, *181*, 219–225.

Saygin, Z. M., Kliemann, D., Iglesias, J. E., van der Kouwe, A. J. W., Boyd, E., Reuter, M., … Alzheimer's Disease Neuroimaging Initiative. (2017). High-resolution magnetic resonance imaging reveals nuclei of the human amygdala: Manual segmentation to automatic atlas. *NeuroImage*, *155*, 370–382.

Schächter, F., Faure-Delanef, L., Guénot, F., Rouger, H., Froguel, P., Lesueur-Ginot, L., & Cohen, D. (1994). Genetic associations with human longevity at the APOE and ACE loci. *Nature Genetics*, *6*, 29–32.

Schoemaker, D., Buss, C., Head, K., Sandman, C. A., Davis, E. P., Chakravarty, M. M., … Pruessner, J. C. (2016). Hippocampus and amygdala volumes from magnetic resonance images in children: Assessing accuracy of FreeSurfer and FSL against manual segmentation. *NeuroImage*, *129*, 1–14.

Schumann, C. M., & Amaral, D. G. (2005). Stereological estimation of the number of neurons in the human amygdaloid complex. *Journal of Comparative Neurology*, *491*, 320–329.

Scott, S. A., DeKosky, S. T., Sparks, D. L., Knox, C. A., & Scheff, S. W. (1992). Amygdala cell loss and atrophy in Alzheimer's disease. *Annals of Neurology*, *32*, 555–563.

Shang, X., Carlson, M. C., & Tang, X. (2018). Quantitative comparisons of three automated methods for estimating intracranial volume: A study of 270 longitudinal magnetic resonance images. *Psychiatry Research: Neuroimaging*, *274*, 23–30.

Soldan, A., Pettigrew, C., Lu, Y., Wang, M. C., Selnes, O., Albert, M., … BIOCARD Research Team. (2015). Relationship of medial temporal lobe atrophy, APOE genotype, and cognitive reserve in preclinical Alzheimer's disease. *Human Brain Mapping*, *36*, 2826–2841.

Sublette, M. E., Baca-Garcia, E., Parsey, R. V., Oquendo, M. A., Rodrigues, S. M., Galfalvy, H., … Mann, J. J. (2008). Effect of BDNF val66met polymorphism on age-related amygdala volume changes in healthy subjects. *Progress in Neuro-Psychopharmacology & Biological Psychiatry*, *32*, 1652–1655.

Swanson, L. W., & Petrovich, G. D. (1998). What is the amygdala? *Trends in Neurosciences*, *21*, 323–331.

Tan, A., Ma, W., Vira, A., Marwha, D., & Eliot, L. (2016). The human hippocampus is not sexually-dimorphic: Meta-analysis of structural MRI volumes. *NeuroImage*, *124*(Pt A), 350–366.

Tyszka, J. M., & Pauli, W. M. (2016). In vivo delineation of subdivisions of the human amygdaloid complex in a high-resolution group template. *Human Brain Mapping*, *37*, 3979–3998.

Vuilleumier, P. (2009). The role of the human amygdala in perception and attention. In P. J. Whalen & E. A. Phelps (Eds.), *The human amygdala* (pp. 220–249). New York: The Guilford Press.

Walhovd, K. B., Fjell, A. M., Reinvang, I., Lundervold, A., Dale, A. M., Eilertsen, D. E., … Fischl, B. (2005). Effects of age on volumes of cortex, white matter and subcortical structures. *Neurobiology of Aging*, *26*, 1261–1270 discussion 1275-8.

Wisdom, N. M., Callahan, J. L., & Hawkins, K. A. (2011). The effects of apolipoprotein E on non-impaired cognitive functioning: A meta-analysis. *Neurobiology of Aging*, *32*, 63–74.

Wright, C. I. (2009). The human amygdala in normal aging and Alzheimer's disease. In P. J. Whalen & E. A. Phelps (Eds.), *The human amygdala* (pp. 382–405). New York: The Guilford Press.

Yamaguchi, N., & Yuri, K. (2012). Changes in oestrogen receptor-β mRNA expression in male rat brain with age. *Journal of Neuroendocrinology*, *24*, 310–318.

Yamaguchi-Shima, N., & Yuri, K. (2007). Age-related changes in the expression of ER-beta mRNA in the female rat brain. *Brain Research*, *1155*, 34–41.

Yesavage, J. A., Brink, T. L., Rose, T. L., Lum, O., Huang, V., Adey, M., & Leirer, V. O. (1982). Development and validation of a geriatric depression screening scale: A preliminary report. *Journal of Psychiatric Research*, *17*, 37–49.

Yilmazer-Hanke, D. M. (2012). Amygdala. In J. K. Mai & G. Paxinos (Eds.), *The human nervous system* (3rd ed., pp. 759–834). London: Elsevier Academic Press.

Ystad, M. A., Lundervold, A. J., Wehling, E., Espeseth, T., Rootwelt, H., Westlye, L. T., … Lundervold, A. (2009). Hippocampal volumes are important predictors for memory function in elderly women. *BMC Medical Imaging*, *22*, 9–17.

Yushkevich, P. A., Piven, J., Hazlett, H. C., Smith, R. G., Ho, S., Gee, J. C., & Gerig, G. (2006). User-guided 3D active contour segmentation of anatomical structures: Significantly improved efficiency and reliability. *NeuroImage*, *31*, 1116–1128.

Ziegler, G., Dahnke, R., Gaser, C., & Alzheimer's Disease Neuroimaging Initiative. (2012). Models of the aging brain structure and individual decline. *Frontiers in Neuroinformatics*, *6*, 3. https://doi.org/10.3389/fninf.2012.00003

How to cite this article: Aghamohammadi-Sereshki A, Hrybouski S, Travis S, et al. Amygdala subnuclei and healthy cognitive aging. *Hum Brain Mapp*. 2019;40:34–52. https://doi.org/10.1002/hbm.24353